


OUTLIER-RESISTANT ROBUST MEDICAL SUPPLY PREPOSITIONING AND REBALANCING IN RESPONSE TO DISASTERS

XUEHONG GAO¹, ZHIJIN CHEN¹, CHANSEOK PARK²,
KANGLIN LIU³ AND QIUHONG ZHAO^{4,5,*}

Abstract. The global impact of severe epidemic outbreaks, exemplified by the coronavirus disease 2019 (COVID-19), has been profound. Consequently, epidemic research has received increasing scholarly attention. Effective control of epidemics and saving lives necessitates the implementation of suitable Medical Supply Prepositioning and Rebalancing (MSPR) strategies. These strategies can facilitate rapid responses and address the dissimilarities in infection prevalence across regions, which result in demand-supply mismatches. However, when the input data used for decision-making contains outliers, the optimal solution may deviate significantly from the true optimal solution obtained from outlier-free input data. Thus, the development of robust optimization methods with outlier-resistant characteristics becomes crucial. In this context, this study utilizes two robust estimators, namely weighted Hodges–Lehmann estimators, and formulates three robust nonlinear mathematical models to address the MSPR problem, which aims to mitigate the adverse effects of data contamination. These models are designed to mitigate the adverse effects of outliers on medical supply allocation decisions, enhancing both efficiency and fairness. Then, a comprehensive case study on the threat of COVID-19 in Hubei province during the early stages of the pandemic was conducted to validate the proposed models and methods. The numerical results demonstrate that the newly proposed robust optimization models outperform traditional methods in terms of outlier resistance, solution stability, and allocation efficiency. Ultimately, this study contributes both theoretically and managerially by offering novel modeling techniques and actionable insights for policymakers and practitioners. It underscores the critical importance of integrating robustness into epidemic supply chain planning and provides practical guidance for developing more resilient, reliable, and equitable medical supply strategies under uncertainty.

Mathematics Subject Classification. 65C60.

Received October 24, 2024. Accepted December 10, 2025.

Keywords. Humanitarian logistics, epidemics, robust optimization, weighted Hodges–Lehmann.

¹ Research Institute of Macro-Safety Science, University of Science and Technology Beijing, Beijing, P.R. China.

² Department of Industrial Engineering, Pusan National University, Busan, Republic of Korea.

³ School of Traffic and Transportation, Beijing Jiaotong University, Beijing, P.R. China.

⁴ School of Economics and Management, Beihang University, Beijing, P.R. China.

⁵ Beijing Key Laboratory of Emergency Support Simulation Technologies for City Operations, Beijing, P.R. China.

*Corresponding author: qhzhao@buaa.edu.cn

1. INTRODUCTION

Over the past decade, a range of natural and man-made disasters, including earthquakes, pandemics, floods, nuclear leaks, and hurricanes, have had a profound impact on various regions, inflicting human suffering and substantial economic losses worldwide. Despite the presence of advanced response mechanisms, one of the most significant threats to society sustainable development remains a critical epidemic. As of August 2021, the coronavirus disease 2019 (COVID-19) had affected more than 200 countries, sparking a surge in the demand for medical supplies and resulting in severe shortages in affected regions. In the absence of well-conceived and efficient plans to facilitate the repositioning and rebalancing of medical supplies, the populations in these areas remain at a heightened risk.

In practice, the ability to effectively respond to epidemic outbreaks hinges largely on the ready availability of medical supplies close to affected areas and the implementation of post-disaster rebalancing strategies for these supplies. On the one hand, owing to hysteretic vaccines, repositioning such medical supplies in appropriate locations is one of the fastest ways to respond, minimizing economic loss and saving lives as much as possible. Achieving this entails the careful design of a well-structured relief network prior to any disaster occurrence. A notable example of an organization adept at this practice is the American Red Cross, a prominent not-for-profit entity dedicated to providing relief services in the aftermath of disasters. Among its regular activities, the American Red Cross emphasizes the repositioning of resources aimed at assisting individuals temporarily displaced by disasters. Typically, these resources are meticulously prepared and stored in advance, then strategically positioned across specific locations within a given region to alleviate the suffering of those affected by the disaster.

In response to epidemic situations, repositioning strategies typically entail the establishment of multiple relief warehouses and cabin hospitals in potential locations. Additionally, the strategy involves the deployment and maintenance of both permanent and temporary stockpiles of medical supplies, with precise quantities, strategically located. Subsequently, a network of connections is established, linking suppliers to demand points to effectively respond to epidemic outbreaks. Following this, an appropriate rebalancing strategy is implemented to efficiently redistribute medical supplies to regions experiencing high demand. One notable challenge in managing epidemic outbreaks lies in the uncertainty surrounding the number of infected cases, a factor influenced by a complex array of variables. Notably, there is a variation in the severity of outbreaks due to differences in infection prevalence across affected regions [24]. Additionally, infected cases are dynamically and unevenly distributed, as observed in the context of COVID-19 [31, 37]. Consequently, the task of repositioning and rebalancing medical supplies in the face of demand uncertainty, through the design of an appropriate relief network, presents a particularly daunting challenge.

In general, the design of an applicable relief network for the repositioning and rebalancing of medical supplies assumes the absence of outliers (*i.e.*, contaminated data). However, in the context of disasters, this foundational assumption is frequently compromised. The data used for decision-making are often collected under volatile or hurried conditions, leading to data contamination (*i.e.*, outliers) and subsequently, variations in solution performance. When the collected uncertain data are tainted by outliers, the optimal solution tends to diverge significantly from the true optimum. For a deeper understanding of the impact of outliers, please refer to the following studies [18, 24, 35, 43–45, 56, 57]. Given data suspected to contain outliers, decisions related to relief efforts should be made using robust methods to ensure both the accuracy and resilience of the solution when addressing humanitarian logistics concerns. Consequently, a robust approach is imperative to mitigate the influence of outliers and uncertainties in data. Therefore, our focus centers on the design of a relief network for medical supply repositioning and rebalancing (MSPR) in scenarios involving data contamination. We propose a corresponding robust optimization model that integrates decisions related to facility location, medical supply repositioning, rebalancing, and medical supply flows. Considering the aforementioned considerations, four critical questions necessitate examination.

- (i) *What key considerations should be addressed when dealing with the MSPR problem in response to epidemics?*
- (ii) *What robust strategies can effectively tackle the MSPR problem in the presence of data uncertainty and outliers?*
- (iii) *How can the robustness of the proposed methods be rigorously evaluated?*
- (iv) *What approaches should be employed to formulate and solve the proposed robust nonlinear optimization models?*

To the best of our knowledge, these four questions have remained largely unexplored in prior research efforts. To bridge these gaps, this study presents four primary contributions with a large-scale extension of our previous study [24]. Firstly, this study addresses a critical aspect often overlooked in humanitarian operations, which is the presence of data uncertainty and outliers in parametric values when tackling the MSPR problem. Secondly, this study introduces two novel robust estimators designed to mitigate the disruptive effects of outliers within an uncertain demand set. Additionally, this study presents four nonlinear optimization models, complementing existing methods in this domain. Thirdly, this study defines a utility metric for quantifying the performance of medical supply rebalancing, particularly focusing on fairness within the MSPR problem. Lastly, the corresponding linearization approaches are developed for the proposed nonlinear optimization models. To validate the efficacy of these contributions, the study investigates the robustness of the newly introduced estimators and conducts a numerical analysis based on a real-world case study. Furthermore, the proposed methodologies are compared with existing ones, clearly demonstrating their superior performance in addressing the MSPR problem under outlier conditions.

The remainder of this paper is structured as follows: Section 2 reviews prior literature concerning the prepositioning and rebalancing of relief resources in disaster response, as well as robust theories for handling data contamination. Section 3 offers an exhaustive description of the MSPR problem and delineates the primary concerns addressed in this study. Section 4 introduces robust nonlinear optimization models for formulating the MSPR problem in the presence of data contamination, along with the accompanying linearization strategies. Section 5 presents a comprehensive case study to validate the proposed models and methods, followed by a thorough examination of extensive numerical experiments and their outcomes. Finally, Section 6 presents conclusions, highlighting contributions, limitations, and future directions.

2. LITERATURE REVIEW

As this study primarily addresses the MSPR problem in the context of uncertainty and outliers, we introduce three main streams of studies.

2.1. MSPR problem in disaster response

Numerous studies have been undertaken to explore a range of challenges within humanitarian operations, including topics such as humanitarian network design, multi-facility location problems, and prepositioning or distribution of commodities. From the standpoint of the disaster “life cycle”, relief operations are typically categorized into two distinct phases: pre- and post-disaster operations.

To mitigate the lengthy shipping times of emergency supplies to disaster-affected areas, substantial research effort has been devoted to pre-disaster operations. For instance, Hong *et al.* [29] developed a pre-disaster relief network, strategically determining facility locations of varying sizes to stock relief supplies for disaster preparedness. Ni *et al.* [39] developed a robust optimization model to address the location and emergency inventory pre-positioning problem considering uncertainties. Arnette *et al.* [4] emphasized the importance of well-planned prepositioning assets for timely relief provisions before a natural disaster strikes, and introduced a mixed-integer linear programming model to determine the locations of emergency shelters for stockpiling assets. Hu *et al.* [30] introduced a two-stage stochastic optimization model to determine supplier selection, facility locations, inventory, and the distribution of relief supplies. Erbeyoğlu *et al.* [17] designed a humanitarian network that strategically determined the locations of distribution centers and the storage of critical supplies in preparation

for disaster management. Moreover, in previous research, significant attention has been devoted to post-disaster operations. For instance, Nagurney *et al.* [38] focused on providing relief supplies to disaster-affected demand points in a post-disaster context, incorporating a generalized Nash equilibrium network. Liu, Lei, *et al.* [33] addressed a multi-period multi-commodity distribution problem using a rolling horizon-based framework, yielding robust relief distribution plans for post-disaster relief efforts. Gao, Jin, *et al.* [23] centered their attention on the rebalancing and transportation of commodities *via* a multimodal transportation system following large-scale natural disasters. Wang *et al.* [60] presented a novel multi-period, data-driven, distributionally robust facility location and capacity planning model during disaster relief, where it was reformulated as a Mixed-Integer Second-Order Cone Program.

During an epidemic outbreak, the sharply increasing transmission of the virus leads to a significant surge in the demand for medical supplies [31]. Consequently, maintaining a sufficient stock of medical supplies in strategically located warehouses becomes pivotal in mitigating the post-epidemic repercussions. However, due to the uneven prevalence of infection across regions, the severity of the epidemic can differ widely [24]. Aligning the medical supply prepositioning strategy with the complex reality often results in a supply-demand imbalance [24]. In such scenarios, remedial measures, such as medical supply rebalancing, become imperative to rectify the discrepancies between supply and demand for medical resources. Hence, the MSPR problem must be solved urgently by designing a proper humanitarian relief network. Cao *et al.* [9] designed an effective reverse logistics supply chain to control virus transmission and promotes a sustainable waste management system, where a bi-level optimization model was formulated to maximize total job opportunities and minimize total costs at the first level, and minimize total infection risks at the second level.

2.2. Data uncertainty with outliers

As discussed in Section 2.1, this study focuses on the prepositioning and rebalancing of medical supplies during both pre-epidemic and post-epidemic periods. Notably, these two periods exhibit distinct characteristics; the data collected during the pre-epidemic period are generally deterministic, in contrast to the inherent uncertainty surrounding data collected post-epidemic. Consequently, each phase of humanitarian operations necessitates a different set of considerations.

The Susceptible-Exposed-Infected-Recovered (SEIR) model, a renowned epidemiological model, establishes a substantial correlation between the number of infected cases and critical parameters. Given that medical supply prepositioning occurs immediately prior to the outbreak awareness, it becomes essential to obtain the demand of the infected cases based solely on the SEIR model, without external epidemic prevention and control measures. However, during epidemic outbreaks, the distribution of infected cases is dynamic and uneven, driven by a multitude of factors that contribute to symptomatic and asymptomatic infections, further amplifying the virus spread [31]. Consequently, after a large-scale disaster, the demand for relief items is usually uncertain. In response to this challenge, considerable research efforts have been dedicated to addressing data uncertainty and aligning it with the realities of disaster environments within the realm of humanitarian operations [8, 11, 13, 14, 19, 59]. Undoubtedly, data uncertainty presents a significant hurdle in decision-making within humanitarian logistics.

While the post-disaster data are inherently uncertain, it is typically assumed that the collected information is free from outliers. However, the complex and chaotic post-disaster environment often results in data being collected under personal preferences or volatile operational conditions [22, 40, 47], leading to data uncertainty that includes outliers. This form of data contamination has garnered considerable attention [18, 21, 35, 45–47]. Nevertheless, the intersection of data uncertainty with outliers in parametric values has remained a relatively underexplored territory within the realm of humanitarian operations. This study aims to address the unique challenges posed by the combination of data uncertainty and outliers.

2.3. Robust strategies in disaster response

Due to the inherent information uncertainty prevalent in disaster response scenarios, numerous robust optimization models have been developed. Typically, previous studies have widely adopted three main categories

of robust strategies. The first category centers on formulating the optimization model under the worst-case scenario, while the other two categories focus on minimizing regret or cost within a specific scenario [12, 34, 36]. These strategies are designed under the assumption that the data used for supporting decision-making have no outliers. However, the rush to respond to a disaster, often occurring under volatile operational conditions or personal preferences, frequently results in the acquisition of uncertain information fraught with outliers [25]. For a comprehensive understanding of the impact of contaminated data on estimator behavior, please refer to the studies developed by Park [43], Gao and Jin [22], Park *et al.* [46], and the more recent work by Gao *et al.* [24]. In such scenarios, traditional scenario-based robust optimization models for decision-making may prove inadequate, as they are grounded in inaccurate information. To mitigate the adverse effects of outliers, the application of high-quality robust estimators emerges as an efficient alternative, ensuring both accuracy and enhancing robustness. For further insights, please consult the study by Park *et al.* [46] and Gao *et al.* [25].

In response to this challenge, the imperative is to develop a robust strategy that exhibits reduced sensitivity to outliers, a facet that has garnered insufficient attention in the context of humanitarian operations. Limited prior studies have explored this aspect. Notably, Gao and Jin [22] delved into the realm of uncertain demand coupled with data contamination, while Gao and Cui [21] pioneered a robust method aimed at mitigating the influence of data contamination within demand point data. Specifically, they employed a (weighted) median as an alternative to a weighted mean to estimate uncertain elements. However, it is worth noting that the (weighted) median-based robust strategy may not be universally effective, as it directly excludes certain scenarios from the uncertain elements. In an endeavor to enhance robust performance, this study adopts a weighted Hodges–Lehmann-based robust strategy, chosen for its reduced bias when compared to other robust estimators [47]. To the best of our knowledge, no prior effort has been undertaken to investigate these novel, adaptable, and robust approaches designed to address the MSPR problem under conditions of uncertainty, especially when tainted by outliers.

2.4. Summary

As presented in Table 1, a comprehensive summary of relevant studies conducted over the past five years is provided. Herein, we compare the primary concerns addressed in these studies with those of previous research efforts, elucidating the research gaps and the novelty inherent in this study. Notably, as shown in Table 1, the MSPR challenges arising from epidemic situations have remained relatively underexplored, primarily due to the distinct nature of such events, which differ significantly from traditional disaster or supply chain scenarios. While several studies have investigated MSPR under general uncertainty, few have specifically accounted for the complex, dynamic, and large-scale disruptions introduced by epidemics. Furthermore, this study delves into the intricate ramifications of both uncertain information and data contamination, areas that are still in their nascent stages of exploration. Existing literature often assumes that the available data is accurate and reliable, neglecting the possibility of systematic errors, incomplete reporting, or deliberate manipulation – issues that are especially prevalent during crises like pandemics. By explicitly modeling data contamination and quantifying its impact on decision-making, our work addresses a critical gap that has substantial practical implications for robust and resilient planning. Additionally, in contrast to prior investigations, we introduce a relatively underemphasized fairness criterion, the law of diminishing marginal utility (DMU), to ensure that resources are allocated more equitably and efficiently. While conventional approaches typically focus on efficiency or cost minimization alone, they often overlook the diminishing benefits of allocating excessive resources to a single entity at the expense of others. Incorporating the DMU criterion allows us to better capture social welfare considerations and achieve a more balanced trade-off between efficiency and fairness, which is crucial in emergency or resource-constrained contexts.

Given the above research gaps, this study makes four main contributions to the literature and practice. First, this study focuses on delineating the principal concerns and establishing an optimal response strategy within the MSPR problem, particularly under conditions where the information collected is both uncertain and contaminated. Second, to mitigate the influence of data contamination on the solution quality, we propose two innovative robust estimators specifically designed for the MSPR context. These estimators enhance the resilience

TABLE 1. Summary of the literature related to the main concerns in humanitarian operations.

Article	Main problem	Epidemics	Uncertainty	Data contamination	Law of DMU	Approach
Stauffer <i>et al.</i> [53]	Asset supply network design	Not	Not	Not	Not	Exact method
Baharmand <i>et al.</i> [6]	Facility location determination	Not	Included	Not	Not	Exact method
Balcik <i>et al.</i> [7]	Pre-positioning network design	Not	Included	Not	Not	Exact method
Arnette <i>et al.</i> [4]	Relief asset pre-positioning	Not	Included	Not	Not	Exact method
Enayati <i>et al.</i> [16]	Influenza vaccine distribution	Included	Not	Not	Not	Exact method
Gao and Cao [20]	Commodity rebalancing	Not	Included	Not	Not	Exact method
Zhang <i>et al.</i> [63]	Medical supply stock and reserve	Included	Included	Not	Not	Exact method
Gao and Cui [21]	Facility location determination	Not	Included	Included	Not	Exact method
Zhang <i>et al.</i> [62]	Relief distribution network design	Not	Included	Not	Not	Exact method
Shokr <i>et al.</i> [52]	Humanitarian relief chain design	Not	Included	Not	Not	Exact method
Paret <i>et al.</i> [42]	Spontaneous volunteer assignment	Not	Included	Not	Not	Heuristic
Stienen <i>et al.</i> [54]	Facility location problem	Not	Included	Not	Not	Exact method
Paul <i>et al.</i> [48]	Recovery planning management	Included	Included	Not	Not	Heuristic
Khoshsirat <i>et al.</i> [32]	Buyer and seller coordination	Included	Included	Not	Not	Exact method
Alem <i>et al.</i> [2]	Humanitarian supply chain design	Included	Included	Not	Not	Heuristic
Wang <i>et al.</i> [58]	Disaster relief management	Not	Included	Not	Not	Exact method
Ransikarbum <i>et al.</i> [49]	Humanitarian logistics planning	Not	Included	Not	Not	Heuristic
Cheng <i>et al.</i> [12]	Fixed-charge location problem	Not	Included	Not	Not	Exact method
Gao <i>et al.</i> [24]	Medical staff rebalancing	Included	Included	Not	Not	Exact method
Ash <i>et al.</i> [5]	Healthcare supply chain resilience	Included	Included	Not	Not	Exact method
Amjadian <i>et al.</i> [3]	Closed-loop supply chain	Not	Included	Not	Not	Exact method
Pamucar <i>et al.</i> [41]	Supplier selection in the relief supply chain	Included	Included	Not	Not	Exact method
Yang <i>et al.</i> [61]	Location-allocation resources	Not	Included	Not	Not	Exact method
Ehsani <i>et al.</i> [15]	Humanitarian logistics network design	Included	Included	Not	Not	Exact method
Sadeghi <i>et al.</i> [50]	Vehicle routing problem	Not	Not	Not	Not	Heuristic
Gharai <i>et al.</i> [26]	Reliable inventory problem	Not	Not	Not	Not	Exact method
Taleizadeh <i>et al.</i> [55]	Supply chain coordination	Not	Not	Not	Not	Heuristic
Gharai <i>et al.</i> [27]	Buyer-vendor problem	Not	Included	Not	Not	Exact method
Cao <i>et al.</i> [9]	Location and transportation problem	Included	Not	Not	Not	Exact method
Wang <i>et al.</i> [60]	Facility location and capacity planning	Not	Included	Not	Not	Exact method
This study	MSPR problem	Included	Included	Included	Included	Exact method

of the decision models by effectively reducing the impact of outliers, erroneous reports, and biased observations. Third, we formulate several robust nonlinear optimization models that capture the essential features of the MSPR problem while incorporating both uncertainty and contamination effects. These models are designed to reflect realistic operational constraints and objectives, providing a more faithful representation of complex decision environments. To make these models practically solvable, we also develop corresponding linearization methods that transform the nonlinear formulations into tractable forms, enabling the computation of globally optimal solutions efficiently. Finally, the proposed methodologies are validated through a comprehensive real-world case study, which demonstrates their superior performance in mitigating the adverse effects of data contamination and uncertainty.

3. PROBLEM DESCRIPTION

3.1. MSPR process

As part of the preparations for an epidemic outbreak, the prepositioning of medical supplies in strategically chosen warehouses is a critical endeavor to ensure the prompt distribution of essential resources, particularly personal protective equipment, throughout the established transportation network (Phase I). Consequently, the identification of warehouse locations within the existing transportation network for the maintenance of medical supply stockpiles serves as a proactive measure to mitigate the post-epidemic ramifications. Hence, the development of a well-structured relief network geared towards the prepositioning of medical supplies emerges as an imperative response to epidemic scenarios. Typically, the distribution of infected cases during an epidemic is neither uniform nor consistent across regions. Additionally, aligning the medical supply prepositioning strategy with the dynamic realities of an epidemic proves to be a formidable challenge, often resulting in a pronounced

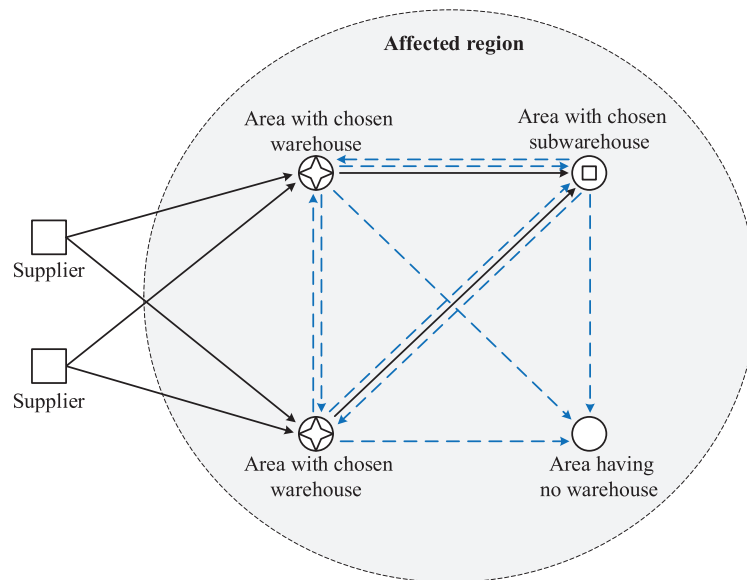


FIGURE 1. A conceptual framework of relief network incorporating the MSPR problem.

imbalance between supply and demand. In this context, the subsequent task of rebalancing medical supplies following the epidemic peak (Phase II) poses yet another complex challenge. To elucidate the key processes inherent in the MSPR problem, a visual representation of the relief network employed in this study is presented in Figure 1.

As depicted in Figure 1, the relief network adopted for this study presents a unique combination of vertical and parallel structures, meticulously designed to correspond with the various stages of the MSPR processes. In this integrated framework, resources are transported from suppliers to warehouses and, subsequently, from suppliers to subwarehouses *via* the intermediary warehouses, all facilitated by the vertical transportation network (illustrated by the solid black arrows in Fig. 1). Please note that the categorization of warehouses and subwarehouses is predetermined based on either administrative hierarchies or the population sizes of the respective regions. In this arrangement, subwarehouses receive direct support from the warehouses. Following the outbreak of an epidemic, the distribution of resources undergoes a transformation *via* the parallel transportation network (represented by the dotted blue arrows in Fig. 1), optimized to ensure swift and efficient delivery within the affected region. Consequently, the primary objectives encompass the strategic selection of optimal warehouse and subwarehouse locations from a pool of potential candidate sites, alongside the determination of the corresponding quantities of stocked medical supplies. The subsequent phase involves the critical task of resource rebalancing, necessitating the calculation of medical supply flows between the various warehouses.

3.2. Data uncertainty with contamination

The virus, whose information is little known in the early stages of an epidemic, leads to highly uncertain information about infected cases because of a series of multifaceted factors. To clarify data uncertainty and outliers, an illustrative example is provided. When dealing with a dataset consisting of several observations, each representing different demand scenarios for medical supplies, the identification of an observation significantly deviating from the others, either exceptionally large or exceptionally small, suggests the presence of an outlier; that is

$$x_i \ll \mathcal{S}/\{x_i\} \text{ or } x_i \gg \mathcal{S}/\{x_i\}. \quad (1)$$

The dataset may contain two or more such outliers, albeit in small proportions. It is imperative to recognize that data contaminated by outliers can lead to biased results. Hence, developing robust methodologies to mitigate the influence of outliers is an essential endeavor. Consequently, the incorporation of both data uncertainty and outliers into the MSPR problem is a practical yet intricate approach, necessitating innovative solutions to address the associated challenges.

3.3. Presumptions

Before presenting the methodology employed to address the MSPR problem under conditions of uncertainty with outliers, four key hypotheses were formulated: (i) It is assumed that the probabilities of scenarios are uniform across all areas (states or cities), thereby simplifying and enhancing the clarity of the proposed mathematical models. (ii) To account for the relative independence of foreseeable situations before and after epidemic events (*i.e.*, during the repositioning and rebalancing phases), two distinct sets of scenarios are considered. (iii) The hypothesis posits that data contamination occurs predominantly after the outbreak of an epidemic. The potential reason is data contamination or anomalies could also arise during the early or mid-epidemic phases, due to factors such as reporting delays, misclassification, or incomplete information. However, in the first stage, decision makers have enough resources to check the accuracy of the data. (iv) The study assumes that the DMU function, linked to uncertain demand within each area, is known. However, it is worth noting that this function can be developed and adjusted to align with practical circumstances. It is pertinent to mention that the development and adaptation of the DMU function to reflect real-world conditions aligns with established practices in research, as observed in studies such as studies [1, 10, 24, 37].

4. METHODOLOGY

4.1. Notations

This study provides partial notations below.

Set notations

\mathcal{S}	Set of suppliers, $s \in \mathcal{S}$;
\mathcal{P}	Set of affected regions, $p \in \mathcal{P}$;
\mathcal{W}	Set of regions with potential warehouses, indexed by $w, v \in \mathcal{W}$, such that $\mathcal{W} \in \mathcal{P}$;
\mathcal{B}	Set of regions with potential subwarehouses, indexed by $b, d \in \mathcal{B}$, such that $\mathcal{B} \in \mathcal{P}$, $\mathcal{W} \cap \mathcal{B} = \emptyset$;
\mathcal{T}	Set of medical-item types, $t \in \mathcal{T}$;
Ξ	Set of scenarios before an epidemic outbreak (Phase I), $\xi \in \Xi$;
Π	Set of scenarios after an epidemic outbreak (Phase II), $\zeta \in \Pi$;

Parameters notations

I_{ts}	Supply of medical-item t from supplier s ;
C_{tw}	Capacity of medical-item t in potential warehouse in region w ;
C_{tb}	Capacity of medical-item t in potential subwarehouse in region b ;
D_{sw}	Distance from supplier s to warehouse in region w ;
D_{wv}	Distance from warehouse in region w to warehouse in region v ;
D_{wb}	Distance from warehouse in region w to subwarehouse in region b ;
D_{bd}	Distance from subwarehouse in region b to subwarehouse in region d ;
S_{sw}	Shipping cost from supplier s to warehouse in region w ;
S_{wb}	Shipping cost from warehouse in region w to subwarehouse in region b ;
O_w	Cost of opening the warehouse in region w ;
O_b	Cost of opening subwarehouse in region b ;

Uncertain elements

- $B_{tw\xi}$ Estimated demand of medical-item t in region w before an epidemic outbreak in scenario ξ ;
- $B_{tb\xi}$ Estimated demand of medical-item t in region b before an epidemic outbreak in scenario ξ ;
- $A_{tw\zeta}$ Estimated demand of medical-item t in region w after an epidemic outbreak in scenario ζ ;
- $A_{tb\zeta}$ Estimated demand of medical-item t in region b after an epidemic outbreak in scenario ζ ;
- T_{wv} Transportation time from warehouse in region w to warehouse in region v ;
- T_{wb} Transportation time from warehouse in region w to subwarehouse in region b ;
- T_{bw} Transportation time from subwarehouse in region b to warehouse in region w ;
- T_{bd} Transportation time from subwarehouse in region b to subwarehouse in region d ;
- P_ξ Probability of scenario ξ in Phase I;
- Q_ζ Probability of scenario ζ in Phase II;
- \mathbb{B} Budget of medical supplies preposition process.

Decision variables

- u_w $\begin{cases} 1 & \text{if warehouse } w \text{ is selected} \\ 0 & \text{otherwise} \end{cases}$
- v_b $\begin{cases} 1 & \text{if subwarehouse } b \text{ is selected} \\ 0 & \text{otherwise} \end{cases}$
- q_{tw} Quantity of stocked medical item t in warehouse in region w before an epidemic outbreak;
- q_{tb} Quantity of stocked medical item t in subwarehouse in region b before an epidemic outbreak;
- o_{tw} Outgoing shipment of medical item t from region w with respect to its stock level;
- r_{tw} Incoming shipment of medical item t in region w ;
- o_{tb} Outgoing shipment of medical item t from region b with respect to its stock level;
- r_{tb} Incoming shipment of medical item t in region b ;
- f_{tsw} Flow of medical item t from supplier s to warehouse in region w ;
- f_{twb} Flow of medical item t from warehouse in region w to subwarehouse in region b ;
- f_{twv} Flow of medical item t from warehouse in region w to warehouse in region v ;
- f_{twb} Flow of medical item t from warehouse in region w to subwarehouse in region b ;
- f_{tbw} Flow of medical item t from subwarehouse in region b to warehouse in region w ;
- f_{tbd} Flow of medical item t from subwarehouse in region b to subwarehouse in region d ;

Other notations

- $M_t(x)$ Marginal diminishing marginal utility function for medical item t ;
- $T_t(x)$ Total diminishing marginal utility function for medical item t ;
- ΔT The change in the total diminishing marginal utilities;
- Ψ_1 The first objective function of maximizing total utility in prepositioning medical supplies;
- Ψ_2 The second objective function of maximizing total utility in rebalancing medical supplies;
- Ψ_3 The third objective function of minimizing total transportation time in rebalancing medical supplies;
- Ψ_2° The second objective function based on traditional HL estimator;
- $\Psi_2^{\circ\circ}$ The second objective function based on traditional WHL1 estimator;
- $\Psi_2^{\circ\circ\circ}$ The second objective function based on traditional WHL2 estimator;
- \mathcal{L} The tri-level sequential multi-objective stochastic optimization model;
- \mathcal{R}_1 The robust tri-level optimization model based on HL estimator;
- \mathcal{R}_2 The robust tri-level optimization model based on WHL1 estimator;
- \mathcal{R}_3 The robust tri-level optimization model based on WHL2 estimator;
- \mathcal{L}^\blacksquare Linearized model based on model \mathcal{L} ;
- $\mathcal{R}_1^\blacksquare$ Linearized model based on model \mathcal{R}_1 ;
- $\mathcal{R}_2^\blacksquare$ Linearized model based on model \mathcal{R}_2 ;

- $\mathcal{R}_3^\blacksquare$ Linearized model based on model \mathcal{R}_3 ;
- Υ_{tw} Outgoing-shipment deviation ratio of medical item t in region w ;
- Υ_{tb} Outgoing-shipment deviation ratio of medical item t in region b ;
- ϑ_{tw} Incoming-shipment deviation ratio of medical item t in region w ;
- ϑ_{tb} Incoming-shipment deviation ratio of medical item t in region b .

4.2. Objective functions

This study centers its attention on the MSPR process, encompassing various objectives. Specifically, the prepositioning of medical supplies primarily revolves around the pursuit of fairness, aiming to maximize utility while adhering to budget constraints prior to an epidemic outbreak. Conversely, during the medical supply rebalancing phase, the objectives encompass both fairness (maximization of utility) and the minimization of transportation time. Detailed elaborations of the objective functions are provided in the subsequent sections.

(1) Maximization of total DMU

In the assessment of fairness, the comprehensive measure employed is the total DMU value, which encompasses distinct DMU functions for each category of medical supplies. It is crucial to highlight that the marginal utility function utilized in this study is based on the unmet demand value associated with each regional unit of medical supplies. For a given medical item t , the marginal and total diminishing marginal utilities are functions of x , represented by $\mathbb{M}_t(x)$ and $\mathbb{T}_t(x)$, respectively. In particular, the change in the total DMU ($\Delta\mathbb{T}$) of medical item t from state x_1 to state x_2 is given in equation (2).

$$\Delta\mathbb{T} = \mathbb{T}_t(x_2) - \mathbb{T}_t(x_1) = \int_{x_1}^{x_2} \mathbb{M}_t(x) dx. \tag{2}$$

Accordingly, the objective function of prepositioning medical supplies is given as follows:

$$\Psi_1 = \text{Max} \sum_{w \in \mathcal{W}} \sum_{t \in \mathcal{T}} \sum_{\xi \in \Xi} P_\xi \int_0^{q_{tw}} \mathbb{M}_{tw\xi}(x) dx + \sum_{b \in \mathcal{B}} \sum_{t \in \mathcal{T}} \sum_{\xi \in \Xi} P_\xi \int_0^{q_{tb}} \mathbb{M}_{tb\xi}(x) dx \tag{3}$$

where $\mathbb{M}_{tw\xi}(x)$ and $\mathbb{M}_{tb\xi}(x)$ are the DMU functions for medial-item t in regions with potential warehouses and subwarehouses, respectively, in scenario ξ .

Lemma 1. *When the quantity of supply of medical item t is significantly less than the demand, the objective function is always positive.*

Proof. It suffices to show the following equation

$$\Psi_1 = \sum_{w \in \mathcal{W}} \sum_{t \in \mathcal{T}} \sum_{\xi \in \Xi} P_\xi \int_0^{q_{tw}} \mathbb{M}_{tw\xi}(x) dx + \sum_{b \in \mathcal{B}} \sum_{t \in \mathcal{T}} \sum_{\xi \in \Xi} P_\xi \int_0^{q_{tb}} \mathbb{M}_{tb\xi}(x) dx > 0, \tag{4}$$

while $q_{tw} > 0$, $q_{tb} > 0$, or both q_{tw} and q_{tb} are positive. □

In accordance with the fundamental tenet of the law of DMU, the initial unit of good consumption or service tends to yield greater utility than subsequent units, with diminishing returns for each additional unit. For a specific medical item t within a given scenario ξ and region w , this principle is embodied in the law of DMU function denoted as $\mathbb{M}_{tw\xi}(x)$. It is worth noting that the availability of medical supplies is constrained (*i.e.*, $q_{tb} < AD$), where AD is the expected demand that equates to a DMU of 0. Consequently, the law of DMU function $\mathbb{M}_{tw\xi}(x)$ consistently maintains positive values for x greater than 0, and the aggregate increase in utility across all scenarios can be expressed as follows:

$$\sum_{\xi \in \Xi} P_\xi \int_0^{q_{tw}} \mathbb{M}_{tw\xi}(x) dx > 0 \quad \forall t \in \mathcal{T}, w \in \mathcal{W}. \tag{5}$$

Similarly, this principle extends to the total DMU function $\mathbb{M}_{tw\xi}(x)$ for x greater than 0. Thus, we establish conclusively that the objective function consistently maintains positive values when the quantity of supply falls short of the expected demand.

The optimization of the medical supply prepositioning strategy is a meticulous process, as it affords ample time for optimal decision-making prior to an epidemic outbreak. However, in the face of an epidemic, immediate response becomes imperative, even in the absence of comprehensive information. In such a scenario, the presence of uncertainty is inevitable, leading us to formulate the second objective function for rebalancing medical supplies as follows:

$$\Psi_2 = \text{Max} \sum_{w \in \mathcal{W}} \sum_{t \in \mathcal{T}} \sum_{\zeta \in \Pi} P_\zeta \int_{q_{tw}^*}^{q_{tw}^* - \sigma_{tw} + r_{tw}} \mathbb{M}'_{tw\zeta}(x) dx + \sum_{b \in \mathcal{B}} \sum_{t \in \mathcal{T}} \sum_{\zeta \in \Pi} P_\zeta \int_{q_{tb}^*}^{q_{tb}^* - \sigma_{tb} + r_{tb}} \mathbb{M}'_{tb\zeta}(x) dx \quad (6)$$

where $\mathbb{M}'_{tw\zeta}(x) dx$ and $\mathbb{M}'_{tb\zeta}(x) dx$ are the DMU functions in regions w and b in scenario ζ , respectively. And q_{tw}^* and q_{tb}^* are the optimal quantities of stocked medical item t in warehouses and subwarehouses, respectively.

Beyond the objectives of optimizing the prepositioning and rebalancing of medical supplies to maximize total utilities before and after an epidemic outbreak, there exists a concurrent imperative to expedite the delivery of medical supplies to assist infected cases promptly. The third objective function seeks to minimize the total transportation time required for the distribution of medical supplies across diverse regions, and it is expressed as follows:

$$\Psi_3 = \text{Min} \sum_{w \in \mathcal{W}} \sum_{v \in \mathcal{V}} \sum_{t \in \mathcal{T}} T_{wv} f_{twv} + \sum_{w \in \mathcal{W}} \sum_{b \in \mathcal{B}} \sum_{t \in \mathcal{T}} T_{wb} f_{twb} + \sum_{b \in \mathcal{B}} \sum_{v \in \mathcal{V}} \sum_{t \in \mathcal{T}} T_{bv} f_{tbv} + \sum_{b \in \mathcal{B}} \sum_{d \in \mathcal{D}} \sum_{t \in \mathcal{T}} T_{bd} f_{tbd}. \quad (7)$$

4.3. Robust methodology

As previously noted, the post-epidemic uncertainty surrounding the number of infections poses a formidable challenge in the prepositioning and rebalancing of medical supplies. Furthermore, the presence of outliers can significantly deviate the solution from the true optimum [24]. To address the issue of data contamination in the context of rebalancing medical supplies, it becomes imperative to develop location estimators that are resilient to outliers. In pursuit of enhanced robustness, several such estimators have been formulated in prior studies [46, 51]. Among these, the HL estimator is defined as the median of pairwise averages of sample observations [28]. This estimator is known for its robustness and efficiency under symmetric distributions, as it reduces the influence of extreme values while still reflecting the central tendency of the data.

Building on this idea, the WHL1 estimator extends the HL estimator by incorporating weights into the pairwise averages. Specifically, it computes all possible pairwise weighted averages of the sample observations and then takes the median of these weighted averages. The weighting scheme allows the estimator to account for differences in the reliability or importance of individual observations, making it more adaptable in situations where data quality varies. Further refining this approach, the WHL2 estimator also starts by computing all pairwise weighted averages but instead of taking a simple median, it calculates a weighted median of these pairwise weighted averages. This additional weighting in the final aggregation step provides even greater flexibility to emphasize certain observations or mitigate the influence of outliers more effectively. These two weighted variants (WHL1 and WHL2) are designed to maintain the robustness of the HL estimator while enhancing its ability to handle contaminated or heterogeneous data by explicitly incorporating weights reflecting data quality or other domain knowledge. For a comprehensive explanation of the formulation, properties, and implementation of the WHL1 and WHL2 estimators, interested readers are referred to the study conducted by Gao *et al.* [25], which introduces and analyzes these estimators in detail, including their theoretical underpinnings and empirical performance.

The HL estimator can be effectively employed to address the uncertainty surrounding DMU values and mitigate the impact of outliers. In this context, each particular realization of the DMU value is treated as an individual observation. To the best of our knowledge, the HL estimator has not been applied in optimization

models designed to tackle uncertain future events characterized by the presence of outliers. By utilizing leveraging the established HL estimator, we can reformulate the second objective function in the following manner:

$$\Psi_2^\circ = \text{Max} \sum_{w \in \mathcal{W}} \sum_{t \in \mathcal{T}} \int_{q_{tw}^*}^{q_{tw}^* - \sigma_{tw} + r_{tw}} \mathbb{M}'_{tw}(x)^\circ dx + \sum_{b \in \mathcal{B}} \sum_{t \in \mathcal{T}} \int_{q_{tb}^*}^{q_{tb}^* - \sigma_{tb} + r_{tb}} \mathbb{M}'_{tb}(x)^\circ dx \quad (8)$$

where $\mathbb{M}'_{tw}(x)^\circ$ and $\mathbb{M}'_{tb}(x)^\circ$ are DMU functions based on the HL estimator in regions w and b , respectively.

In traditional HL estimation, uncertain future events are not assigned weights (*i.e.*, probabilities). Recognizing the importance of incorporating these probabilities, we introduce the WHL1 and WHL2 estimators. Consequently, this study employs the WHL1 and WHL2 estimators as substitutes for the HL estimator when addressing uncertain future events with associated weights.

With the WHL1 estimator developed by Gao *et al.* [25], the second objective function is reformulated as follows:

$$\Psi_2^{\circ\circ} = \text{Max} \sum_{w \in \mathcal{W}} \sum_{t \in \mathcal{T}} \int_{q_{tw}^*}^{q_{tw}^* - \sigma_{tw} + r_{tw}} \mathbb{M}'_{tw}(x)^{\circ\circ} dx + \sum_{b \in \mathcal{B}} \sum_{t \in \mathcal{T}} \int_{q_{tb}^*}^{q_{tb}^* - \sigma_{tb} + r_{tb}} \mathbb{M}'_{tb}(x)^{\circ\circ} dx \quad (9)$$

where $\mathbb{M}'_{tw}(x)^{\circ\circ}$ and $\mathbb{M}'_{tb}(x)^{\circ\circ}$ are DMU functions based on the WHL1 estimator in regions w and b , respectively.

With the WHL2 estimator developed by Gao *et al.* [25], the second objective function is given as follows:

$$\Psi_2^{\circ\circ\circ} = \text{Max} \sum_{w \in \mathcal{W}} \sum_{t \in \mathcal{T}} \int_{q_{tw}^*}^{q_{tw}^* - \sigma_{tw} + r_{tw}} \mathbb{M}'_{tw}(x)^{\circ\circ\circ} dx + \sum_{b \in \mathcal{B}} \sum_{t \in \mathcal{T}} \int_{q_{tb}^*}^{q_{tb}^* - \sigma_{tb} + r_{tb}} \mathbb{M}'_{tb}(x)^{\circ\circ\circ} dx \quad (10)$$

where $\mathbb{M}'_{tw}(x)^{\circ\circ\circ}$ and $\mathbb{M}'_{tb}(x)^{\circ\circ\circ}$ are DMU functions based on the WHL2 estimator in regions w and b , respectively.

4.4. Mathematical models

In this subsection, we introduce several tri-level nonlinear mathematical models. The first model is developed using the traditional scenario-based stochastic approach. Furthermore, this study presents three robust optimization models aimed at mitigating the influence of outliers.

(1) Stochastic mathematical model

With uncertain demand, a tri-level sequential multi-objective stochastic optimization model \mathcal{L} is proposed, which is given by

\mathcal{L} :

$$\begin{aligned} \Psi_1 = \text{Max} & \sum_{w \in \mathcal{W}} \sum_{t \in \mathcal{T}} \sum_{\xi \in \Xi} P_\xi \int_0^{q_{tw}} \mathbb{M}_{tw\xi}(x) dx \\ & + \sum_{b \in \mathcal{B}} \sum_{t \in \mathcal{T}} \sum_{\xi \in \Xi} P_\xi \int_0^{q_{tb}} \mathbb{M}_{tb\xi}(x) dx \end{aligned} \quad (11)$$

s.t.

$$\sum_{s \in \mathcal{S}} I_{ts} = \sum_{w \in \mathcal{W}} q_{tw} + \sum_{b \in \mathcal{B}} q_{tb} \quad \forall t \in \mathcal{T} \quad (12)$$

$$\sum_{s \in \mathcal{S}} \sum_{t \in \mathcal{T}} f_{tsw} = q_{tw} \leq C_{tw} \quad \forall t \in \mathcal{T}, w \in \mathcal{W} \quad (13)$$

$$\sum_{w \in \mathcal{W}} \sum_{t \in \mathcal{T}} f_{twb} = q_{tb} \leq C_{tb} \quad \forall t \in \mathcal{T}, b \in \mathcal{B} \quad (14)$$

$$\sum_{s \in \mathcal{S}} \sum_{t \in \mathcal{T}} f_{tsw} = q_{tw} \leq \mathbb{M}u_w \quad \forall t \in \mathcal{T}, w \in \mathcal{W} \quad (15)$$

$$\sum_{w \in \mathcal{W}} \sum_{t \in \mathcal{T}} f_{twb} = q_{tb} \leq \mathbb{M}v_b \quad \forall t \in \mathcal{T}, b \in \mathcal{B} \quad (16)$$

$$\begin{aligned} & \sum_{w \in \mathcal{W}} O_w u_w + \sum_{b \in \mathcal{B}} O_b v_b \\ & + \sum_{s \in \mathcal{S}} \sum_{w \in \mathcal{W}} \sum_{t \in \mathcal{T}} D_{sw} S_{sw} f_{tsw} + \sum_{w \in \mathcal{W}} \sum_{b \in \mathcal{B}} \sum_{t \in \mathcal{T}} D_{wb} S_{sw} f_{twb} \leq \mathbb{B} \end{aligned} \quad (17)$$

$$q_{tw} \text{ and } q_{tb} \text{ are non-negative integer variables} \quad \forall t \in \mathcal{T}, w \in \mathcal{W}, b \in \mathcal{B} \quad (18)$$

$$\begin{aligned} \arg \Psi_2 = \text{Max} & \sum_{w \in \mathcal{W}} \sum_{t \in \mathcal{T}} \sum_{\zeta \in \Pi} P_\zeta \int_{q_{tw}^*}^{q_{tw}^* - o_{tw} + r_{tw}} \mathbb{M}'_{tw\zeta}(x) dx \\ & + \sum_{b \in \mathcal{B}} \sum_{t \in \mathcal{T}} \sum_{\zeta \in \Pi} P_\zeta \int_{q_{tb}^*}^{q_{tb}^* - o_{tb} + r_{tb}} \mathbb{M}'_{tb\zeta}(x) dx \end{aligned} \quad (19)$$

$$\sum_{w \in \mathcal{W}} o_{tw} + \sum_{b \in \mathcal{B}} o_{tb} = \sum_{w \in \mathcal{W}} r_{tw} + \sum_{b \in \mathcal{B}} r_{tb} \quad \forall t \in \mathcal{T} \quad (20)$$

$$o_{tw} \leq q_{tw}^*, o_{tb} \leq q_{tb}^* \quad \forall t \in \mathcal{T}, w \in \mathcal{W}, b \in \mathcal{B} \quad (21)$$

$$r_{tw} + q_{tw}^* \leq \max\{A_{tw1}, A_{tw2}, \dots\}, r_{tb} + q_{tb}^* \leq \max\{A_{tb1}, A_{tb2}, \dots\} \quad \forall t \in \mathcal{T}, w \in \mathcal{W}, b \in \mathcal{B} \quad (22)$$

$$\begin{aligned} \arg \Psi_3 = \text{Min} & \sum_{w \in \mathcal{W}} \sum_{v \in \mathcal{W}} \sum_{t \in \mathcal{T}} T_{wv} f_{twv} + \sum_{w \in \mathcal{W}} \sum_{b \in \mathcal{B}} \sum_{t \in \mathcal{T}} T_{wb} f_{twb} \\ & + \sum_{b \in \mathcal{B}} \sum_{v \in \mathcal{W}} \sum_{t \in \mathcal{T}} T_{bv} f_{tbv} + \sum_{b \in \mathcal{B}} \sum_{d \in \mathcal{B}} \sum_{t \in \mathcal{T}} T_{bd} f_{tbd} \end{aligned} \quad (23)$$

$$\sum_{v \in \mathcal{W}} f_{twv} + \sum_{b \in \mathcal{B}} f_{twb} \leq o_{tw}^* \quad \forall t \in \mathcal{T}, w \in \mathcal{W} \quad (24)$$

$$\sum_{v \in \mathcal{W}} f_{tbv} + \sum_{d \in \mathcal{B}} f_{tbd} \leq o_{tb}^* \quad \forall t \in \mathcal{T}, b \in \mathcal{B} \quad (25)$$

$$\sum_{w \in \mathcal{W}} f_{twv} + \sum_{b \in \mathcal{B}} f_{tbv} \geq r_{tv}^* \quad \forall t \in \mathcal{T}, v \in \mathcal{W} \quad (26)$$

$$\sum_{w \in \mathcal{W}} f_{twb} + \sum_{b \in \mathcal{B}} f_{tbd} \geq r_{td}^* \quad \forall t \in \mathcal{T}, d \in \mathcal{B}. \quad (27)$$

The upper-level objective function (11) seeks to maximize the total expected DMU by prepositioning medical supplies in Phase I. Constraint (12) aims to ensure a balance between the supplied and received medical supplies. Constraints (13) and (14) impose limitations on the quantities of received medical supplies, ensuring they do not exceed the capacities of the warehouses and subwarehouses in regions w and b , respectively. It is important to note that this study considers capacities on a per-medical-item basis, taking into account their unique reserve conditions to achieve an efficient global optimum. Constraints (15) and (16) ensure that no medical supplies are allocated to unopened warehouses in regions w and b , respectively. Constraint (17) represents the budget constraint, while Constraint (18) defines the decision variables. Equation (19) forms the middle-level objective function, which aims to maximize the total expected DMU by rebalancing medical supplies in Phase II. This objective is subject to Constraints (20)–(22), where the optimal decisions (q_{tw}^* and q_{tb}^*) obtained from the upper-level problem serve as input parameters in the middle-level problem. Constraint (20) ensures a balance between the supplied and received shipments. Constraint (21) restricts the quantities of outgoing medical supplies to be less than the stocked levels in regions w and b . Constraint (22) limits the quantities of the received medical supplies to be less than the maximum demand in regions w and b . Equation (23) defines

the lower-level objective function, which aims to minimize the total transportation time for the transport of medical supplies. This objective is subject to Constraints (24)–(27), which ensure the transportation balance of medical supplies among different regions. The optimal solution $(\phi_{tw}^*, \phi_{tb}^*, r_{tw}^*, \text{ and } r_{td}^*)$ obtained from the middle-level problem is used as input for the lower-level problem. It is worth noting that the warehouse and subwarehouse notations defined in the medical supply prepositioning process are also applicable in the medical supply rebalancing process, as regions without warehouses are identical to regions with warehouses having zero stock levels of medical supplies.

(2) HL-enabled robust mathematical model

Because uncertain information is likely to be associated with data contamination, a robust tri-level optimization model \mathcal{R}_1 is required. To address this, the HL-enabled robust mathematical model is provided, in which the HL is used rather than the weighted mean.

$\mathcal{R}_1 :$

Ψ_1

s.t.

Constraints (12)–(18)

$$\arg \Psi_2^\circ = \text{Max} \sum_{w \in \mathcal{W}} \sum_{t \in \mathcal{T}} \int_{q_{tw}^*}^{q_{tw}^* - \phi_{tw} + r_{tw}} \mathbb{M}'_{tw}(x)^\circ dx + \sum_{b \in \mathcal{B}} \sum_{t \in \mathcal{T}} \int_{q_{tb}^*}^{q_{tb}^* - \phi_{tb} + r_{tb}} \mathbb{M}'_{tb}(x)^\circ dx \tag{28}$$

Constraints (20)–(22)

$\arg \Psi_3$

Constraints (24)–(27)

where $\mathbb{M}'_{tw}(x)^\circ$ and $\mathbb{M}'_{tb}(x)^\circ$ are the DMU functions based on the HL estimator in regions w and b , respectively.

(3) WHL1-enabled robust mathematical model

Because the possible demand realizations are associated with probabilities, using WHL1 is more appropriate than HL as the WHL1 incorporates weights into consideration. The WHL1-enabled robust mathematical model \mathcal{R}_2 is given below.

$\mathcal{R}_2 :$

Ψ_1

s.t.

Constraints (12)–(18)

$$\arg \Psi_2^{\circ\circ} = \text{Max} \sum_{w \in \mathcal{W}} \sum_{t \in \mathcal{T}} \int_{q_{tw}^*}^{q_{tw}^* - \phi_{tw} + r_{tw}} \mathbb{M}'_{tw}(x)^{\circ\circ} dx + \sum_{b \in \mathcal{B}} \sum_{t \in \mathcal{T}} \int_{q_{tb}^*}^{q_{tb}^* - \phi_{tb} + r_{tb}} \mathbb{M}'_{tb}(x)^{\circ\circ} dx \tag{29}$$

Constraints (20)–(22)

$\arg \Psi_3$

Constraints (24)–(27)

where $\mathbb{M}'_{tw}(x)^{\circ\circ}$ and $\mathbb{M}'_{tb}(x)^{\circ\circ}$ are the DMU functions based on the WHL1 in regions w and b , respectively.

(4) WHL2-enabled robust optimization model

In addition, this study formulates a WHL2-enabled robust optimization model as the WHL2 estimator contains more information on data uncertainty than WHL1. The WHL2-enabled robust optimization model \mathcal{R}_3 is presented below.

$\mathcal{R}_3 :$

Ψ_1

s.t.

Constraints (12)–(18)

$$\arg \Psi_2^{\circ\circ\circ} = \text{Max} \sum_{w \in \mathcal{W}} \sum_{t \in \mathcal{T}} \int_{q_{tw}^*}^{q_{tw}^* - o_{tw} + r_{tw}} M'_{tw}(x)^{\circ\circ\circ} dx + \sum_{b \in \mathcal{B}} \sum_{t \in \mathcal{T}} \int_{q_{tb}^*}^{q_{tb}^* - o_{tb} + r_{tb}} M'_{tb}(x)^{\circ\circ\circ} dx \quad (30)$$

Constraints (20)–(22)

$\arg \Psi_3$

Constraints (24)–(27)

where $M'_{tw}(x)^{\circ\circ\circ}$ and $M'_{tb}(x)^{\circ\circ\circ}$ are the DMU functions based on the WHL2 in regions w and b , respectively.

4.5. Linearization approach

The mathematical models proposed above are nonlinear owing to (11), (19), and (28)–(30), making it impossible to solve and obtain the global optimum in their current forms. To achieve the global optimum, reformulating the above mathematical models is required to get rid of its nonlinearity by introducing some new auxiliary parameters and variables. This adjustment allows for their solution using the IBM CPLEX Optimizer. Specifically, this study introduces six auxiliary parameters into the model, which are given by

$nq_{tw}^{(+i)}$ Number stocked medical item t in warehouse in region w before an epidemic outbreak.

$nq_{tb}^{(+i)}$ Number stocked medical item t in sub warehouse in region b before an epidemic outbreak.

$no_{tw}^{(-i)}$ The quantity of outgoing medical item t is i in warehouse in region w after an epidemic outbreak.

$nr_{tw}^{(+i)}$ The quantity of incoming medical item t is in warehouse in region w after an epidemic outbreak.

$no_{tb}^{(-i)}$ The quantity of outgoing medical item t in sub warehouse in region b after an epidemic outbreak.

$nr_{tb}^{(+i)}$ The quantity of incoming medical item t in sub warehouse in region b after an epidemic outbreak.

Then, the optimal discrete solution space in objective functions Ψ_1 and Ψ_2 can be obtained, which is given by

$$\begin{aligned} nq_{tw}^{(+i)} &= 0, \dots, i, \dots, \min\{B_{tw\xi}, C_{tw}\} & \forall t \in \mathcal{T}, w \in \mathcal{W} \\ nq_{tb}^{(+i)} &= 0, \dots, i, \dots, \min\{B_{tb\xi}, C_{tb}\} & \forall t \in \mathcal{T}, b \in \mathcal{B} \\ no_{tw}^{(-i)} &= 0, \dots, i, \dots, q_{tw}^* & \forall t \in \mathcal{T}, w \in \mathcal{W} \\ nr_{tw}^{(+i)} &= 0, \dots, i, \dots, \max_{\zeta} A_{tw\zeta} - q_{tw}^* & \forall t \in \mathcal{T}, w \in \mathcal{W} \\ no_{tb}^{(-i)} &= 0, \dots, i, \dots, q_{tb}^* & \forall t \in \mathcal{T}, b \in \mathcal{B} \\ nr_{tb}^{(+i)} &= 0, \dots, i, \dots, \max_{\zeta} A_{tb\zeta} - q_{tb}^* & \forall t \in \mathcal{T}, b \in \mathcal{B}. \end{aligned}$$

Subsequently, we introduce six additional binary variables designed to ascertain the ideal quantities of medical item t that should be stocked, dispatched, and received in these regions.

$$bq_{tw}^{(+i)} = \begin{cases} 1 & \text{if the number of stocked item } t \text{ is } i \text{ in region } w \\ 0 & \text{otherwise} \end{cases} \quad \forall t \in \mathcal{T}, w \in \mathcal{W}$$

$$\begin{aligned}
 bq_{tb}^{(+i)} &= \begin{cases} 1 & \text{if the number of stocked item } t \text{ is } i \text{ in region } b \\ 0 & \text{otherwise} \end{cases} & \forall t \in \mathcal{T}, b \in \mathcal{B} \\
 a\sigma_{tw}^{(-i)} &= \begin{cases} 1 & \text{if the number of sent item } t \text{ is } i \text{ in region } w \\ 0 & \text{otherwise} \end{cases} & \forall t \in \mathcal{T}, w \in \mathcal{W} \\
 ar_{tw}^{(+i)} &= \begin{cases} 1 & \text{if the number of received medical item } t \text{ is } i \text{ in region } w \\ 0 & \text{otherwise} \end{cases} & \forall t \in \mathcal{T}, w \in \mathcal{W}. \\
 a\sigma_{tb}^{(-i)} &= \begin{cases} 1 & \text{if the number of sent medical item } t \text{ is } i \text{ in region } b \\ 0 & \text{otherwise} \end{cases} & \forall t \in \mathcal{T}, b \in \mathcal{B} \\
 ar_{tb}^{(+i)} &= \begin{cases} 1 & \text{if the number of received medical item } t \text{ is } i \text{ in region } b \\ 0 & \text{otherwise} \end{cases} & \forall t \in \mathcal{T}, b \in \mathcal{B}.
 \end{aligned}$$

In addition, to further linearize the proposed models, six more auxiliary variables need to be defined, which are given by

$$\begin{aligned}
 xq_{tw}^{(+i)} &= \begin{cases} 1 & \text{if } q_{tw} > nq_{tw}^{(+i)} \\ 0 & \text{otherwise} \end{cases} & \forall t \in \mathcal{T}, w \in \mathcal{W} \\
 xq_{tb}^{(+i)} &= \begin{cases} 1 & \text{if } q_{tb} > nq_{tb}^{(+i)} \\ 0 & \text{otherwise} \end{cases} & \forall t \in \mathcal{T}, b \in \mathcal{B} \\
 y\sigma_{tw}^{(-i)} &= \begin{cases} 1 & \text{if } \sigma_{tw} > n\sigma_{tw}^{(-i)} \\ 0 & \text{otherwise} \end{cases} & \forall t \in \mathcal{T}, w \in \mathcal{W} \\
 yr_{tw}^{(+i)} &= \begin{cases} 1 & \text{if } r_{tw} > nr_{tw}^{(+i)} \\ 0 & \text{otherwise} \end{cases} & \forall t \in \mathcal{T}, w \in \mathcal{W} \\
 z\sigma_{tb}^{(-i)} &= \begin{cases} 1 & \text{if } \sigma_{tb} > n\sigma_{tb}^{(-i)} \\ 0 & \text{otherwise} \end{cases} & \forall t \in \mathcal{T}, b \in \mathcal{B} \\
 zr_{tb}^{(+i)} &= \begin{cases} 1 & \text{if } r_{tb} > nr_{tb}^{(+i)} \\ 0 & \text{otherwise} \end{cases} & \forall t \in \mathcal{T}, b \in \mathcal{B}.
 \end{aligned}$$

(1) Reformulation of the proposed model \mathcal{F} .

The proposed robust optimization model \mathcal{F} can be modified as the below model \mathcal{F}^\blacksquare , which is given by

$$\begin{aligned}
 &Z^\blacksquare : \\
 \Psi_1 = \text{Max} & \sum_{t \in \mathcal{T}} \left[\sum_{w \in \mathcal{W}} \sum_{\xi \in \Xi} P_\xi \sum_{i=0}^{\min\{B_{tw\xi}, C_{tw}\}} M_{tw\xi}(nq_{tw}^{(+i)}) \cdot xq_{tw}^{(+i)} \right. \\
 & \left. + \sum_{b \in \mathcal{B}} \sum_{\xi \in \Xi} P_\xi \sum_{i=0}^{\min\{B_{tb\xi}, C_{tb}\}} M_{tb\xi}(nq_{tb}^{(+i)}) \cdot xq_{tb}^{(+i)} \right] \tag{31}
 \end{aligned}$$

s.t.

Constraints (12)–(18)

$$\sum_{i=0}^{\min\{B_{tw\xi}, C_{tw}\}} bq_{tw}^{(+i)} = 1 \quad \forall t \in \mathcal{T}, w \in \mathcal{W} \tag{32}$$

$$\sum_{i=0}^{\min\{B_{tb\xi}, C_{tb}\}} b q_{tb}^{(+i)} = 1 \quad \forall t \in \mathcal{T}, b \in \mathcal{B} \quad (33)$$

$$q_{tw} = \sum_{i=0}^{\min\{B_{tw\xi}, C_{tw}\}} n q_{tw}^{m(+i)} \cdot b q_{tw}^{(+i)} \quad \forall t \in \mathcal{T}, w \in \mathcal{W} \quad (34)$$

$$q_{tb} = \sum_{i=0}^{\min\{B_{tb\xi}, C_{tb}\}} n q_{tb}^{(+i)} \cdot b q_{tb}^{(+i)} \quad \forall t \in \mathcal{T}, b \in \mathcal{B} \quad (35)$$

$$q_{tw} - n q_{tw}^{(+i)} \geq (x q_{tw}^{(+i)} - 1) \cdot \mathcal{M} \quad \forall t \in \mathcal{T}, w \in \mathcal{W} \quad (36)$$

$$q_{tw} - n q_{tw}^{(+i)} \leq x q_{tw}^{(+i)} \cdot \mathcal{M} \quad \forall t \in \mathcal{T}, w \in \mathcal{W} \quad (37)$$

$$q_{tb} - n q_{tb}^{(+i)} \geq (x q_{tb}^{(+i)} - 1) \cdot \mathcal{M} \quad \forall t \in \mathcal{T}, b \in \mathcal{B} \quad (38)$$

$$q_{tb} - n q_{tb}^{(+i)} \leq x q_{tb}^{(+i)} \cdot \mathcal{M} \quad \forall t \in \mathcal{T}, b \in \mathcal{B} \quad (39)$$

$$\begin{aligned} \arg \Psi_2 = \text{Max} \sum_{t \in \mathcal{T}} \left\{ \sum_{w \in \mathcal{W}} \sum_{\zeta \in \Pi} P_{\zeta} \left[\sum_{i=0}^{\max_{\zeta} A_{tw\zeta} - q_{tw}^*} \mathbb{M}'_{tw\zeta} \left(q_{tw}^* + n r_{tw}^{(+i)} \right) \right. \right. \\ \left. \left. \cdot y r_{tw}^{(+i)} - \sum_{i=0}^{q_{tw}^*} \mathbb{M}'_{tw\zeta} \left(q_{tw}^* - n o_{tw}^{(-i)} \right) \cdot y o_{tw}^{(-i)} \right] \right. \\ \left. + \sum_{b \in \mathcal{B}} \sum_{\zeta \in \Pi} P_{\zeta} \left[\sum_{i=0}^{\max_{\zeta} A_{tb\zeta} - q_{tb}^*} \mathbb{M}'_{tb\zeta} \left(q_{tb}^* + n r_{tb}^{(+i)} \right) \cdot z r_{tb}^{(+i)} \right. \right. \\ \left. \left. - \sum_{i=0}^{q_{tb}^*} \mathbb{M}'_{tb\zeta} \left(q_{tb}^* - n o_{tb}^{(-i)} \right) \cdot z o_{tb}^{(-i)} \right] \right\} \quad (40) \end{aligned}$$

s.t.

Constraints (20)–(23)

$$\sum_{i=0}^{q_{tw}^*} a o_{tw}^{(-i)} = 1 \quad \forall t \in \mathcal{T}, w \in \mathcal{W} \quad (41)$$

$$\sum_{i=0}^{\max_{\zeta} A_{tw\zeta} - q_{tw}^*} a r_{tw}^{(+i)} = 1 \quad \forall t \in \mathcal{T}, w \in \mathcal{W} \quad (42)$$

$$\sum_{i=0}^{q_{tb}^*} a o_{tb}^{(-i)} = 1 \quad \forall t \in \mathcal{T}, b \in \mathcal{B} \quad (43)$$

$$\sum_{i=0}^{\max_{\zeta} A_{tb\zeta} - q_{tb}^*} a r_{tb}^{(+i)} = 1 \quad \forall t \in \mathcal{T}, b \in \mathcal{B} \quad (44)$$

$$o_{tw} = \sum_{i=0}^{q_{tw}^*} n o_{tw}^{(-i)} \cdot a o_{tw}^{(-i)} \quad \forall t \in \mathcal{T}, w \in \mathcal{W} \quad (45)$$

$$r_{tw} = \sum_{i=0}^{\max_{\zeta} A_{tw\zeta} - q_{tw}^*} n r_{tw}^{(+i)} \cdot a r_{tw}^{(+i)} \quad \forall t \in \mathcal{T}, w \in \mathcal{W} \quad (46)$$

$$\sigma_{tb} = \sum_{i=0}^{q_{tb}^*} n\sigma_{tb}^{(-i)} \cdot a\sigma_{tb}^{(-i)} \quad \forall t \in \mathcal{T}, b \in \mathcal{B} \quad (47)$$

$$r_{tb} = \sum_{i=0}^{\max_{\zeta} A_{tb\zeta} - q_{tb}^*} nr_{tb}^{(+i)} \cdot ar_{tb}^{(+i)} \quad \forall t \in \mathcal{T}, b \in \mathcal{B} \quad (48)$$

$$\sigma_{tw} - n\sigma_{tw}^{(-i)} \geq (y\sigma_{tw}^{(-i)} - 1) \cdot \mathcal{M} \quad \forall t \in \mathcal{T}, w \in \mathcal{W} \quad (49)$$

$$\sigma_{tw} - n\sigma_{tw}^{(-i)} \leq y\sigma_{tw}^{(-i)} \cdot \mathcal{M} \quad \forall t \in \mathcal{T}, w \in \mathcal{W} \quad (50)$$

$$r_{tw} - nr_{tw}^{(+i)} \geq (yr_{tw}^{(+i)} - 1) \cdot \mathcal{M} \quad \forall t \in \mathcal{T}, w \in \mathcal{W} \quad (51)$$

$$r_{tw} - nr_{tw}^{(+i)} \leq yr_{tw}^{(+i)} \cdot \mathcal{M} \quad \forall t \in \mathcal{T}, w \in \mathcal{W} \quad (52)$$

$$\sigma_{tb} - n\sigma_{tb}^{(-i)} \geq (z\sigma_{tb}^{(-i)} - 1) \cdot \mathcal{M} \quad \forall t \in \mathcal{T}, b \in \mathcal{B} \quad (53)$$

$$\sigma_{tb} - n\sigma_{tb}^{(-i)} \leq z\sigma_{tb}^{(-i)} \cdot \mathcal{M} \quad \forall t \in \mathcal{T}, b \in \mathcal{B} \quad (54)$$

$$r_{tb} - nr_{tb}^{(+i)} \geq (zr_{tb}^{(+i)} - 1) \cdot \mathcal{M} \quad \forall t \in \mathcal{T}, b \in \mathcal{B} \quad (55)$$

$$r_{tb} - nr_{tb}^{(+i)} \leq zr_{tb}^{(+i)} \cdot \mathcal{M} \quad \forall t \in \mathcal{T}, b \in \mathcal{B} \quad (56)$$

$$\sum_{i=0}^{q_{tw}^*} a\sigma_{tw}^{(-i)} + \sum_{i=0}^{\max_{\zeta} A_{tw\zeta} - q_{tw}^*} ar_{tw}^{(+i)} \leq 1 \quad \forall t \in \mathcal{T}, w \in \mathcal{W} \quad (57)$$

$$\sum_{i=0}^{q_{tb}^*} a\sigma_{tb}^{(-i)} + \sum_{i=0}^{\max_{\zeta} A_{tb\zeta} - q_{tb}^*} ar_{tb}^{(+i)} \leq 1 \quad \forall t \in \mathcal{T}, b \in \mathcal{B} \quad (58)$$

$$\begin{aligned} \arg \Psi_3 = & \text{Min} \sum_{w \in \mathcal{W}} \sum_{v \in \mathcal{W}} \sum_{t \in \mathcal{T}} T_{wv} f_{twv} + \sum_{w \in \mathcal{W}} \sum_{b \in \mathcal{B}} \sum_{t \in \mathcal{T}} T_{wb} f_{twb} \\ & + \sum_{b \in \mathcal{B}} \sum_{v \in \mathcal{W}} \sum_{t \in \mathcal{T}} T_{bv} f_{tbv} + \sum_{b \in \mathcal{B}} \sum_{d \in \mathcal{B}} \sum_{t \in \mathcal{T}} T_{bd} f_{tbd} \end{aligned}$$

Constraints (24)–(27).

The upper-level objective function is the same as the equation (31). Constraints (32) and (33) ensure the unique solution determination from the discrete solution space. Constraints (34) and (35) determine the optimal quantities of stocked medical supplies. Constraints (36) and (37) guarantee that the objective function (31) counts the utility only while $q_{tw} > nq_{tw}^{(+i)}$. Constraints (38) and (39) ensure that the objective function (31) counts only while $q_{tb} > nq_{tb}^{(+i)}$. The middle-level objective function is the same as equation (40). Constraints (41)–(44) guarantee the unique solution determination from the discrete solution space. Constraints (45)–(48) determine the optimal quantities of receiving and sent medical supplies. Constraints (49) and (50) guarantee that the objective function (40) counts the utility only while $\sigma_{tw} > n\sigma_{tw}^{(-i)}$. Constraints (51) and (52) guarantee that the objective function (40) counts the utility only while $r_{tw} > nr_{tw}^{(+i)}$. Constraints (53) and (54) guarantee that the objective function (40) counts the utility only while $\sigma_{tb} > n\sigma_{tb}^{(-i)}$. Constraints (55) and (56) guarantee that the objective function (40) counts the utility only while $r_{tb} > nr_{tb}^{(+i)}$. Constraints (57) and (58) guarantee that only sending or receiving medical supplies could happen.

(2) Reformulation of the proposed model \mathcal{R}_1 .

The proposed robust optimization model \mathcal{R}_1 can be modified as the model $\mathcal{R}_1^\blacksquare$, which is given by

$\mathcal{R}_1^\blacksquare$:

$$\Psi_1 = \text{Max} \sum_{t \in \mathcal{T}} \left[\sum_{w \in \mathcal{W}} \sum_{\xi \in \Xi} P_\xi \sum_{i=0}^{\min\{B_{tw\xi}, C_{tw}\}} \mathbb{M}_{tw\xi} \left(nq_{tw}^{(+i)} \right) \cdot xq_{tw}^{(+i)} + \sum_{b \in \mathcal{B}} \sum_{\xi \in \Xi} P_\xi \sum_{i=0}^{\min\{B_{tb\xi}, C_{tb}\}} \mathbb{M}_{tb\xi} \left(nq_{tb}^{(+i)} \right) \cdot xq_{tb}^{(+i)} \right]$$

s.t.

Constraints (12)–(18), (32)–(39)

$$\begin{aligned} \arg \Psi_2^\circ = \text{Max} \sum_{t \in \mathcal{T}} \left\{ \sum_{w \in \mathcal{W}} \left[\sum_{i=0}^{\max_\zeta A_{tw\zeta} - q_{tw}^*} \mathbb{M}'_{tw\zeta} \left(q_{tw}^* + nr_{tw}^{(+i)} \right)^\circ \cdot yr_{tw}^{(+i)} - \sum_{i=0}^{q_{tw}^*} \mathbb{M}'_{tw\zeta} \left(q_{tw}^* - no_{tw}^{(-i)} \right)^\circ \cdot yo_{tw}^{(-i)} \right] \right. \\ \left. + \sum_{b \in \mathcal{B}} \left[\sum_{i=0}^{\max_\zeta A_{tb\zeta} - q_{tb}^*} \mathbb{M}'_{tb\zeta} \left(q_{tb}^* + nr_{tb}^{(+i)} \right)^\circ \cdot zr_{tb}^{(+i)} - \sum_{i=0}^{q_{tb}^*} \mathbb{M}'_{tb\zeta} \left(q_{tb}^* - no_{tb}^{(-i)} \right)^\circ \cdot zo_{tb}^{(-i)} \right] \right\} \end{aligned} \quad (59)$$

Constraints (20)–(22), (41)–(58)

$$\arg \Psi_3 = \text{Min} \sum_{w \in \mathcal{W}} \sum_{v \in \mathcal{V}} \sum_{t \in \mathcal{T}} T_{wv} f_{twv} + \sum_{w \in \mathcal{W}} \sum_{b \in \mathcal{B}} \sum_{t \in \mathcal{T}} T_{wb} f_{twb} + \sum_{b \in \mathcal{B}} \sum_{v \in \mathcal{V}} \sum_{t \in \mathcal{T}} T_{bv} f_{tbv} + \sum_{b \in \mathcal{B}} \sum_{d \in \mathcal{B}} \sum_{t \in \mathcal{T}} T_{bd} f_{tbd}$$

Constraints (23)–(27).

(3) Reformulation of the proposed model \mathcal{R}_2 .

The proposed robust optimization model \mathcal{R}_2 can be modified as the model $\mathcal{R}_2^\blacksquare$, which is given by

$\mathcal{R}_2^\blacksquare$:

$$\Psi_1 = \text{Max} \sum_{t \in \mathcal{T}} \left[\sum_{w \in \mathcal{W}} \sum_{\xi \in \Xi} P_\xi \sum_{i=0}^{\min\{B_{tw\xi}, C_{tw}\}} \mathbb{M}_{tw\xi} \left(nq_{tw}^{(+i)} \right) \cdot xq_{tw}^{(+i)} + \sum_{b \in \mathcal{B}} \sum_{\xi \in \Xi} P_\xi \sum_{i=0}^{\min\{B_{tb\xi}, C_{tb}\}} \mathbb{M}_{tb\xi} \left(nq_{tb}^{(+i)} \right) \cdot xq_{tb}^{(+i)} \right]$$

s.t.

Constraints (12)–(18), (32)–(39)

$$\begin{aligned} \Psi_2^{\circ\circ} = \text{Max} \sum_{t \in \mathcal{T}} \left\{ \sum_{w \in \mathcal{W}} \left[\sum_{i=0}^{\max_\zeta A_{tw\zeta} - q_{tw}^*} \mathbb{M}'_{tw\zeta} \left(q_{tw}^* + nr_{tw}^{(+i)} \right)^{\circ\circ} \cdot yr_{tw}^{(+i)} - \sum_{i=0}^{q_{tw}^*} \mathbb{M}'_{tw\zeta} \left(q_{tw}^* - no_{tw}^{(-i)} \right)^{\circ\circ} \cdot yo_{tw}^{(-i)} \right] \right. \\ \left. + \sum_{b \in \mathcal{B}} \left[\sum_{i=0}^{\max_\zeta A_{tb\zeta} - q_{tb}^*} \mathbb{M}'_{tb\zeta} \left(q_{tb}^* + nr_{tb}^{(+i)} \right)^{\circ\circ} \cdot zr_{tb}^{(+i)} - \sum_{i=0}^{q_{tb}^*} \mathbb{M}'_{tb\zeta} \left(q_{tb}^* - no_{tb}^{(-i)} \right)^{\circ\circ} \cdot zo_{tb}^{(-i)} \right] \right\} \end{aligned} \quad (60)$$

Constraints (20)–(22), (41)–(58)

$$\arg \Psi_3 = \text{Min} \sum_{w \in \mathcal{W}} \sum_{v \in \mathcal{V}} \sum_{t \in \mathcal{T}} T_{wv} f_{twv} + \sum_{w \in \mathcal{W}} \sum_{b \in \mathcal{B}} \sum_{t \in \mathcal{T}} T_{wb} f_{twb} + \sum_{b \in \mathcal{B}} \sum_{v \in \mathcal{V}} \sum_{t \in \mathcal{T}} T_{bv} f_{tbv} + \sum_{b \in \mathcal{B}} \sum_{d \in \mathcal{B}} \sum_{t \in \mathcal{T}} T_{bd} f_{tbd}$$

Constraints (24)–(27).

(4) Reformulation of the proposed model \mathcal{R}_3 .

The proposed robust optimization model \mathcal{R}_3 can be modified as the model $\mathcal{R}_3^\blacksquare$, which is given by

$\mathcal{R}_3^\blacksquare$:

$$\Psi_1 = \text{Max} \sum_{t \in \mathcal{T}} \left[\sum_{w \in \mathcal{W}} \sum_{\xi \in \Xi} P_\xi \sum_{i=0}^{\min\{B_{tw\xi}, C_{tw}\}} \mathbb{M}_{tw\xi} \left(nq_{tw}^{(+i)} \right) \cdot xq_{tw}^{(+i)} + \sum_{b \in \mathcal{B}} \sum_{\xi \in \Xi} P_\xi \sum_{i=0}^{\min\{B_{tb\xi}, C_{tb}\}} \mathbb{M}_{tb\xi} \left(nq_{tb}^{(+i)} \right) \cdot xq_{tb}^{(+i)} \right]$$

s.t.

Constraints (12)–(18), (32)–(39)

$$\begin{aligned}
 \arg \Psi_2^{\circ\circ} = \text{Max} \sum_{t \in \mathcal{T}} \left\{ \sum_{w \in \mathcal{W}} \left[\sum_{i=0}^{\max_{\zeta} A_{tw\zeta} - \varphi_{tw}^*} \mathbb{M}'_{tw\zeta} \left(\varphi_{tw}^* + n\mathcal{r}_{tw}^{(+i)} \right)^{\circ\circ} \cdot y\mathcal{r}_{tw}^{(+i)} \right. \right. \\
 \left. \left. - \sum_{i=0}^{\varphi_{tw}^*} \mathbb{M}'_{tw\zeta} \left(\varphi_{tw}^* - n\mathcal{o}_{tw}^{(-i)} \right)^{\circ\circ} \cdot y\mathcal{o}_{tw}^{(-i)} \right] \right. \\
 \left. + \sum_{b \in \mathcal{B}} \left[\sum_{i=0}^{\max_{\zeta} A_{tb\zeta} - \varphi_{tb}^*} \mathbb{M}'_{tb\zeta} \left(\varphi_{tb}^* + n\mathcal{r}_{tb}^{(+i)} \right)^{\circ\circ} \cdot y\mathcal{r}_{tb}^{(+i)} \right. \right. \\
 \left. \left. - \sum_{i=0}^{\varphi_{tb}^*} \mathbb{M}'_{tb\zeta} \left(\varphi_{tb}^* - n\mathcal{o}_{tb}^{(-i)} \right)^{\circ\circ} \cdot y\mathcal{o}_{tb}^{(-i)} \right] \right\} \tag{61}
 \end{aligned}$$

Constraints (20)–(22), (41)–(58).

$$\arg \Psi_3 = \text{Min} \sum_{w \in \mathcal{W}} \sum_{v \in \mathcal{V}} \sum_{t \in \mathcal{T}} T_{wv} f_{twv} + \sum_{w \in \mathcal{W}} \sum_{b \in \mathcal{B}} \sum_{t \in \mathcal{T}} T_{wb} f_{twb} + \sum_{b \in \mathcal{B}} \sum_{v \in \mathcal{V}} \sum_{t \in \mathcal{T}} T_{bv} f_{tbv} + \sum_{b \in \mathcal{B}} \sum_{d \in \mathcal{D}} \sum_{t \in \mathcal{T}} T_{bd} f_{tbd}$$

Constraints (24)–(27).

5. CASE STUDY

5.1. Data generation

Regarding the period of COVID-19 exposure, a real case study was conducted to validate the developed methodologies in this study. Three sources of data were utilized as inputs. The first source comprised data from the Medical and Health Channel of the WeChat Official Account, encompassing information on the total number of confirmed cases, deaths, and recoveries. The second source was the official situation report of Hubei Province. The third source was data obtained from the Baidu map (refer to Fig. 2). All datasets have been compiled in our public repository (<https://github.com/Xuehong-Gao/Hubei-Province/issues>). As depicted in Figure 2, we considered 16 regions: Wuhan (WH), Huangshi (HS), Shiyan (SY), Yichang (YC), Xiangyang (XY), Ezhou (EZ), Jingmen (JM), Tianmen (TM), Xiaogan (XG), Qianjiang (QJ), Jingzhou (JZ), Enshi (ES), Huanggang (HG), Xianning (XN), Suizhou (SZ), and Xiantao (XT). Among these regions, those with a population exceeding 5 000 000, namely WH, XY, JZ, and HG, were categorized as warehouses, while the rest were considered sub-warehouses.

For rapid assistance to victims immediately following a large-scale disaster, it is imperative to preposition and store medical supplies at specific locations in advance. Given the unpredictable and unknown locations of epidemic outbreaks, equal treatment of all areas within the affected region is necessary when prepositioning medical supplies. Before the detection of the epidemic, this study assumed a direct linear correlation, denoted as ϖ (unit/population/km²), and used it to estimate the demand for medical supplies based on population density (see scenario constructions associated with probability types T1, T2, and T3 in Tab. 2). Estimating the number of newly infected cases can be quite challenging; thus, this study leveraged the methodology developed by Gao *et al.* [24] to calculate the number of newly infected patients over the following two weeks, thereby determining the DMU functions. In particular, this study presented four possible scenarios associated with two sets of regression rates (C1 and C2) and probability types (T1, T2, and T3) to implement the proposed models (see Tab. 2). To evaluate the outlier-resistance properties of the proposed robust optimization models, this study assumed the use of an arbitrarily large or small value, denoted as \wp , to represent the contaminated realization of a scenario. Investigating the robust performance of the proposed models when exposed to input data with

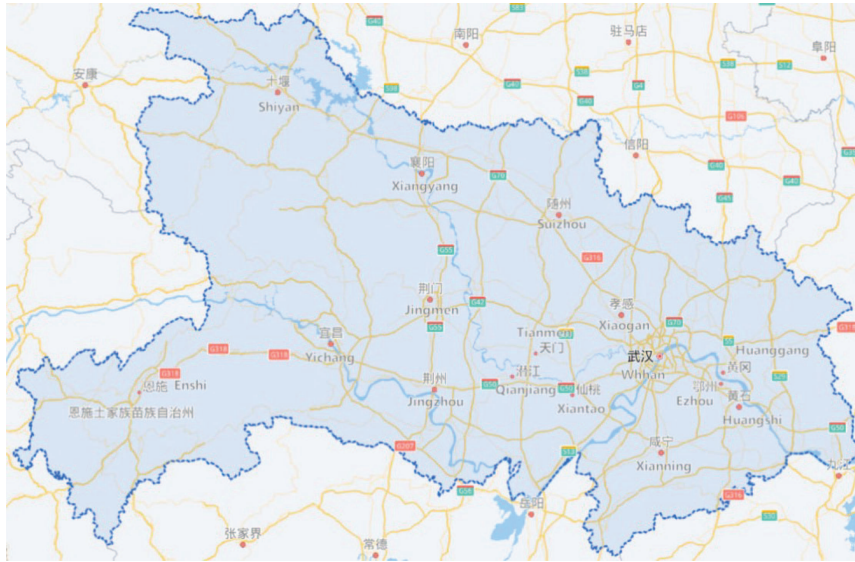


FIGURE 2. Hubei Map with transportation network.

TABLE 2. Scenarios considered in this study.

Process	Instance No.	$\xi = 1$	$\xi = 2$	$\xi = 3$	$\xi = 4$	
		ϖ	60	80	100	120
Medical supply prepositioning (Phase I)	1	T1	$P_1 = 0.4$	$P_2 = 0.3$	$P_3 = 0.2$	$P_4 = 0.1$
	2	T2	$P_1 = 0.2$	$P_2 = 0.3$	$P_3 = 0.3$	$P_4 = 0.2$
	3	T3	$P_1 = 0.1$	$P_2 = 0.2$	$P_3 = 0.3$	$P_4 = 0.4$
Medical supply rebalancing (Phase II)	Instance No.	$\zeta = 1$	$\zeta = 2$	$\zeta = 3$	$\zeta = 4$	
	4	C1	$\rho_1 = 0.75$	$\rho_2 = 0.80$	$\rho_3 = 0.85$	$\rho_4 = 0.90$
		T1	$P_1 = 0.4$	$P_2 = 0.3$	$P_3 = 0.2$	$P_4 = 0.1$
	5	C1	$\rho_1 = 0.75$	$\rho_2 = 0.80$	$\rho_3 = 0.85$	$\rho_4 = 0.90$
		T2	$P_1 = 0.2$	$P_2 = 0.3$	$P_3 = 0.3$	$P_4 = 0.2$
	6	C1	$\rho_1 = 0.75$	$\rho_2 = 0.80$	$\rho_3 = 0.85$	$\rho_4 = 0.90$
		T3	$P_1 = 0.1$	$P_2 = 0.2$	$P_3 = 0.3$	$P_4 = 0.4$
	7	C2	$\rho_1 = 0.85$	$\rho_2 = 0.90$	$\rho_3 = 0.95$	$\rho_4 = 1.00$
		T1	$P_1 = 0.4$	$P_2 = 0.3$	$P_3 = 0.2$	$P_4 = 0.1$
8	C2	$\rho_1 = 0.85$	$\rho_2 = 0.90$	$\rho_3 = 0.95$	$\rho_4 = 1.00$	
	T2	$P_1 = 0.2$	$P_2 = 0.3$	$P_3 = 0.3$	$P_4 = 0.2$	
9	C2	$\rho_1 = 0.85$	$\rho_2 = 0.90$	$\rho_3 = 0.95$	$\rho_4 = 1.00$	
	T3	$P_1 = 0.1$	$P_2 = 0.2$	$P_3 = 0.3$	$P_4 = 0.4$	

outliers allows decision-makers to gain a better understanding of the influence of outliers and make more reliable decisions. The numerical instances were implemented using the CPLEX solver, running on a computer equipped with an 11th Gen Intel(R) Core(TM) i7-11700@2.5 GHz processor and 32 GB of RAM, operating under the Windows 10 Pro system.

5.2. Numerical validation of the upper-level problems (Phase I)

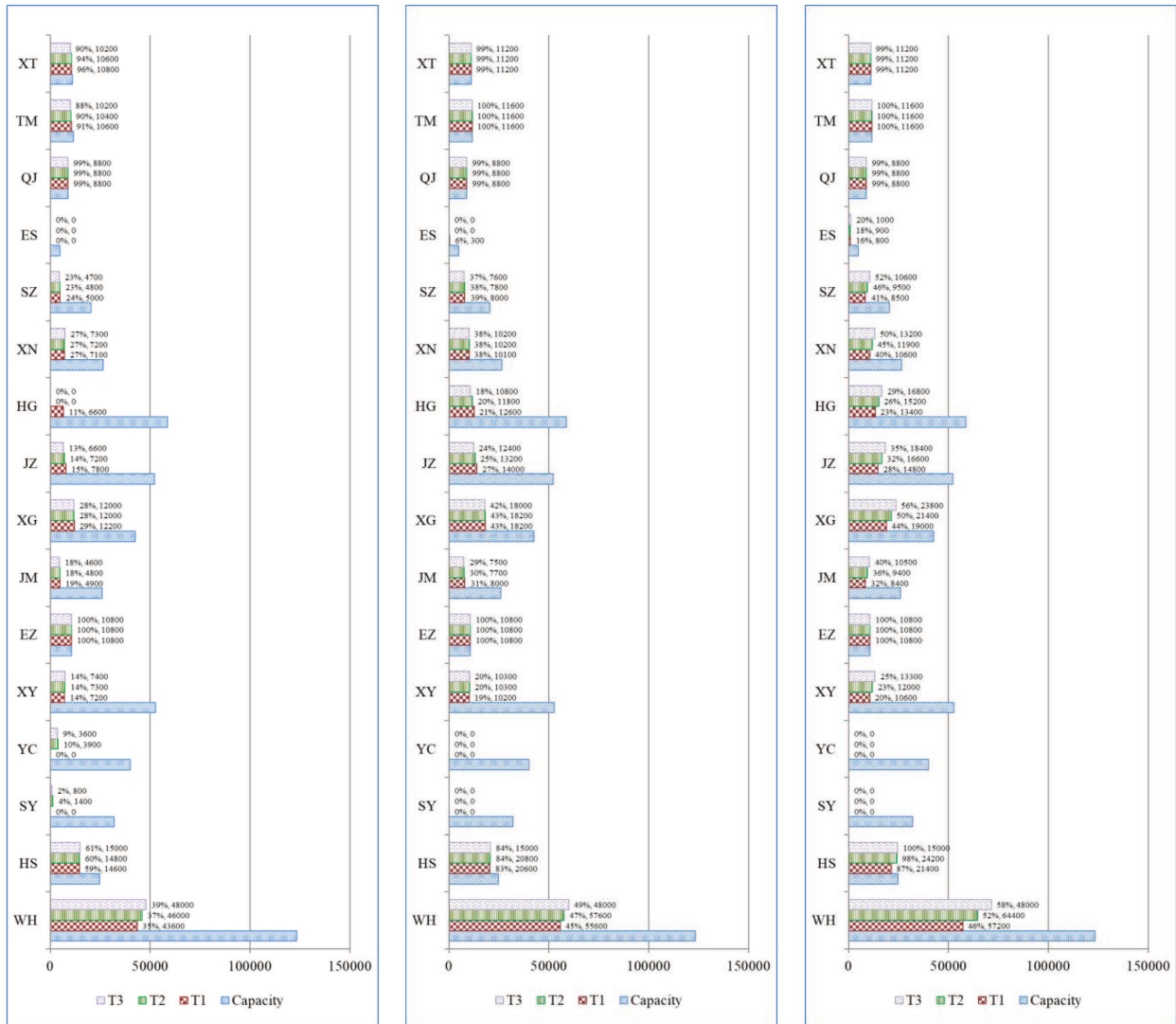
The upper-level problem related to uncertain demand can be effectively solved using CPLEX once the proposed linearization approach has been applied. Given that the primary distinction among the proposed models (\mathcal{L} , \mathcal{R}_1 , \mathcal{R}_2 , and \mathcal{R}_3) resides in the middle-level problem, this study conducted identical numerical experiments to validate the proposed linearization approach and assess computational efficiency. As depicted in Figure 3, the optimal upper-level decision variables, representing stock levels of medical supplies to support infected cases across the 16 regions of Hubei Province, are presented for varying supply quantities from suppliers. The data in Figure 3 reveal a strong correlation between the quantities of stocked medical supplies and factors such as capacity, supply levels, budget constraints, and scenario constructions. Additionally, stocking rates (q_{tw}/C_{tw} and q_{tb}/C_{tb}) for these 16 regions are displayed in Figure 3, assuming capacity limits are based on their population.

This study first explores the impact of capacity on the medical supply prepositioning strategy. In particular, Figure 3 illustrates that only four regions (EZ, QJ, TM, and XT) achieve high stock rates (>85%) relative to overall supply quantities from suppliers and probability constructions. This outcome is attributed to their high investment-output ratios and greater population density, which effectively limit stocked medical supplies in these regions. Conversely, three regions (SY, YC, and ES) remain unopened under general conditions due to budget constraints and lower population density. Notably, the behavior of suppliers significantly influences the final medical supply prepositioning strategy. Specifically, as the supply quantity increases from 300 000 to 500 000, these 16 regions are able to maintain higher stock levels of medical supplies, as evident in Figure 3. Furthermore, budget limitations directly dictate the number of open warehouses and subwarehouses. For instance, when the supply quantity from suppliers remains at 300 000 under probability type T1 (No. 1), three subwarehouses (SY, YC, and ES) are unable to open due to budget constraints. Scenario construction, specifically the choice of probability types, also plays a crucial role in shaping the final medical supply prepositioning strategy. Notably, for WH, the region maintains varying stock levels of medical supplies under different probability types, as depicted in Figure 3. This variation is attributed to the way different probability types emphasize demand for medical supplies. For instance, probability type T3 (No. 3) places a greater emphasis on demand than probability types T1 and T2 (No. 1 and 2), which results in increased demand for medical supplies. Applying probability type T3 (No. 3) to WH encourages greater demand compared to other regions. Moreover, the study found that CPLEX consistently provides optimal solutions for each instance within a 10 s timeframe, affirming the computational efficiency of the proposed linearization approach.

5.3. Numerical validation of the middle- and lower-level problem (Phase II) without outliers

To assess the robustness of the proposed models against outliers, it is imperative to establish the optimal solution under the assumption that the original dataset is devoid of outliers. Once the optimal upper-level decisions for the medical supply prepositioning strategy have been determined, it becomes possible to construct the optimal solutions for the middle- and lower-level problems. Specifically, in order to test the efficacy of the proposed robust methodologies, this subsection focuses on three instances (T1, T2, and T3) with a fixed supply quantity of 400 000. Figures 4 and 5 present the optimal medical supply rebalancing schemes, encompassing incoming and outgoing shipments as well as medical supply flows, for Cases C1 and C2 across the 16 regions. These schemes are designed to maximize the total DMU value (Ψ_2) in the middle-level problem. It is worth noting that only WH is identified as a demand point due to its exceptionally high number of infections, while other regions are treated as supply points, contributing their medical supplies to WH, except for SY and YC. By analyzing the incoming and outgoing shipments in these 16 regions, an optimal transportation scheme can be readily derived, considering Ψ_3 .

To further demonstrate the effectiveness of the proposed models in addressing the MSPR problem without outliers, we conducted a comparison using the same numerical instances. Specifically, we compared medical supply rebalancing strategies by employing four different models (\mathcal{L} , \mathcal{R}_1 , \mathcal{R}_2 , and \mathcal{R}_3) for each instance.



(a) Supply=300,000

(b) Supply=400,000

(c) Supply=500,000

FIGURE 3. Prepositioning strategy and stocking rates given different supply quantities (No. 1–3).

Among these, the robust estimators integrated into models \mathcal{R}_2 and \mathcal{R}_3 are newly proposed in this study and are applied here for the first time in the context of the MSPR problem, representing a methodological innovation over existing approaches. As depicted in Figures 6 and 7, concerning the outgoing and incoming shipments across the 16 regions, the optimal solutions derived from models \mathcal{R}_1 , \mathcal{R}_2 , and \mathcal{R}_3 closely approximate the true optimum achieved by model Z. This observation suggests that the proposed robust models are capable of maintaining high solution quality even under ideal, noise-free conditions, indicating their general applicability and reliability. To provide a more precise assessment, this study introduced deviation ratios, denoted as $(\Upsilon_{tw}$ or $\Upsilon_{tb})$ and $(\vartheta_{tw}$ or $\vartheta_{tb})$, for the optimal outgoing and incoming shipments in two representative regions (WH and HG), respectively.

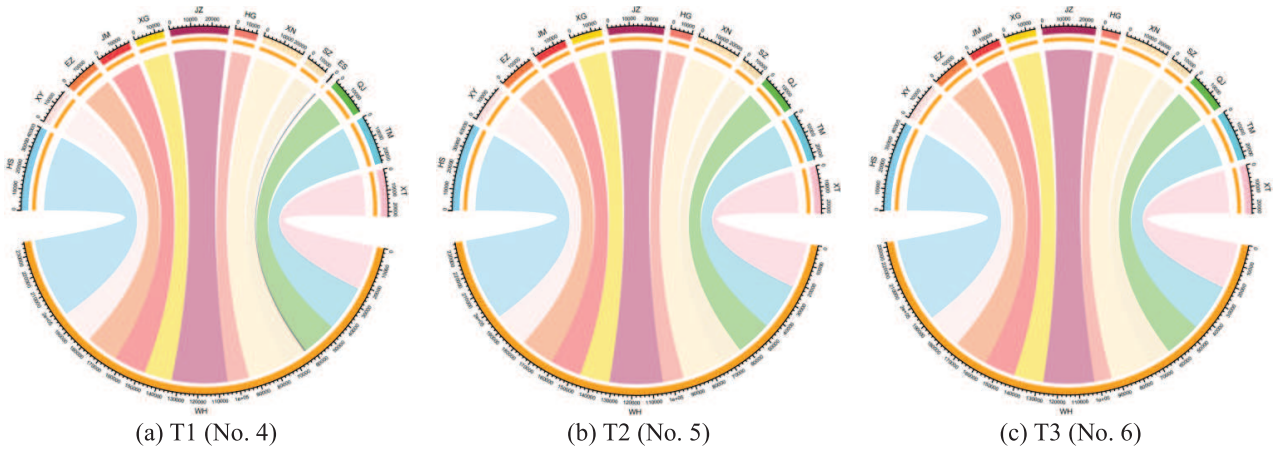


FIGURE 4. Medical supply flows among different regions without outliers in Case C1.

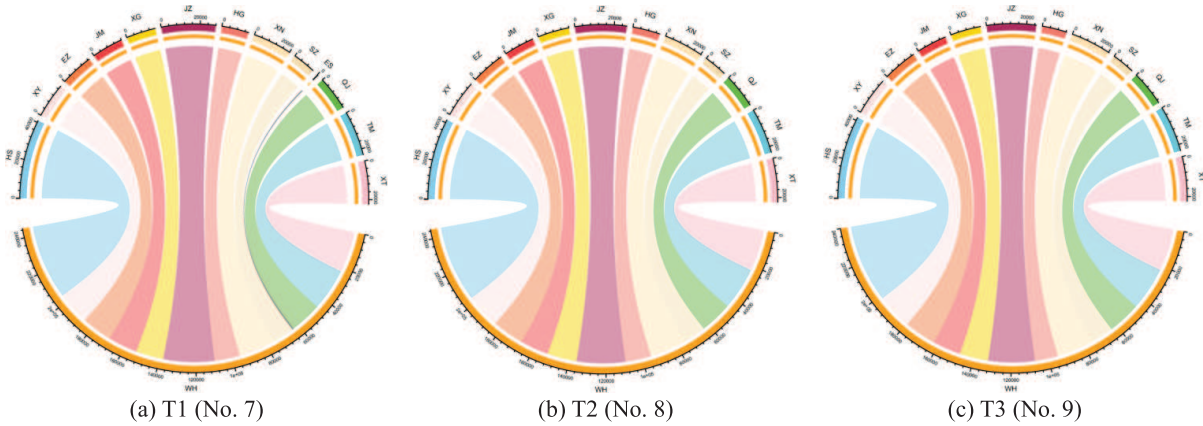


FIGURE 5. Medical supply flows among different regions without outliers in Case C2.

Further details can be found in equations (53) and (54).

$$\Upsilon_{tw} \text{ or } \Upsilon_{tb} = \frac{|\sigma_{tw}(\mathcal{R}_i) - \sigma_{tw}(\mathcal{L})|}{\sigma_{tw}(\mathcal{L})} \text{ or } \frac{|\sigma_{tb}(\mathcal{R}_i) - \sigma_{tb}(\mathcal{L})|}{\sigma_{tb}(\mathcal{L})} \quad i = 1, 2, 3 \quad (53)$$

$$\vartheta_{tw} \text{ or } \vartheta_{tb} = \frac{|\tau_{tw}(\mathcal{R}_i) - \tau_{tw}(\mathcal{L})|}{\tau_{tw}(\mathcal{L})} \text{ or } \frac{|\tau_{tb}(\mathcal{R}_i) - \tau_{tb}(\mathcal{L})|}{\tau_{tb}(\mathcal{L})} \quad i = 1, 2, 3. \quad (54)$$

The numerical results, summarized in Table 3, reveal that the deviation ratios achieved by all three alternative models are exceedingly small, often within negligible margins, thereby affirming their high degree of consistency and interchangeability with the benchmark solution. Notably, a closer examination of these results shows that the robust models \mathcal{R}_2 and \mathcal{R}_3 consistently outperform model \mathcal{R}_1 , exhibiting even smaller deviation ratios across both regions and both shipment directions. This improvement can largely be attributed to the incorporation of weighted robust estimators in \mathcal{R}_2 and \mathcal{R}_3 , which enhances their ability to account for subtle variations in data distribution and better approximate the true optimum. In summary, the comparative analysis highlights that the proposed robust models not only preserve solution quality in the absence of outliers but also surpass

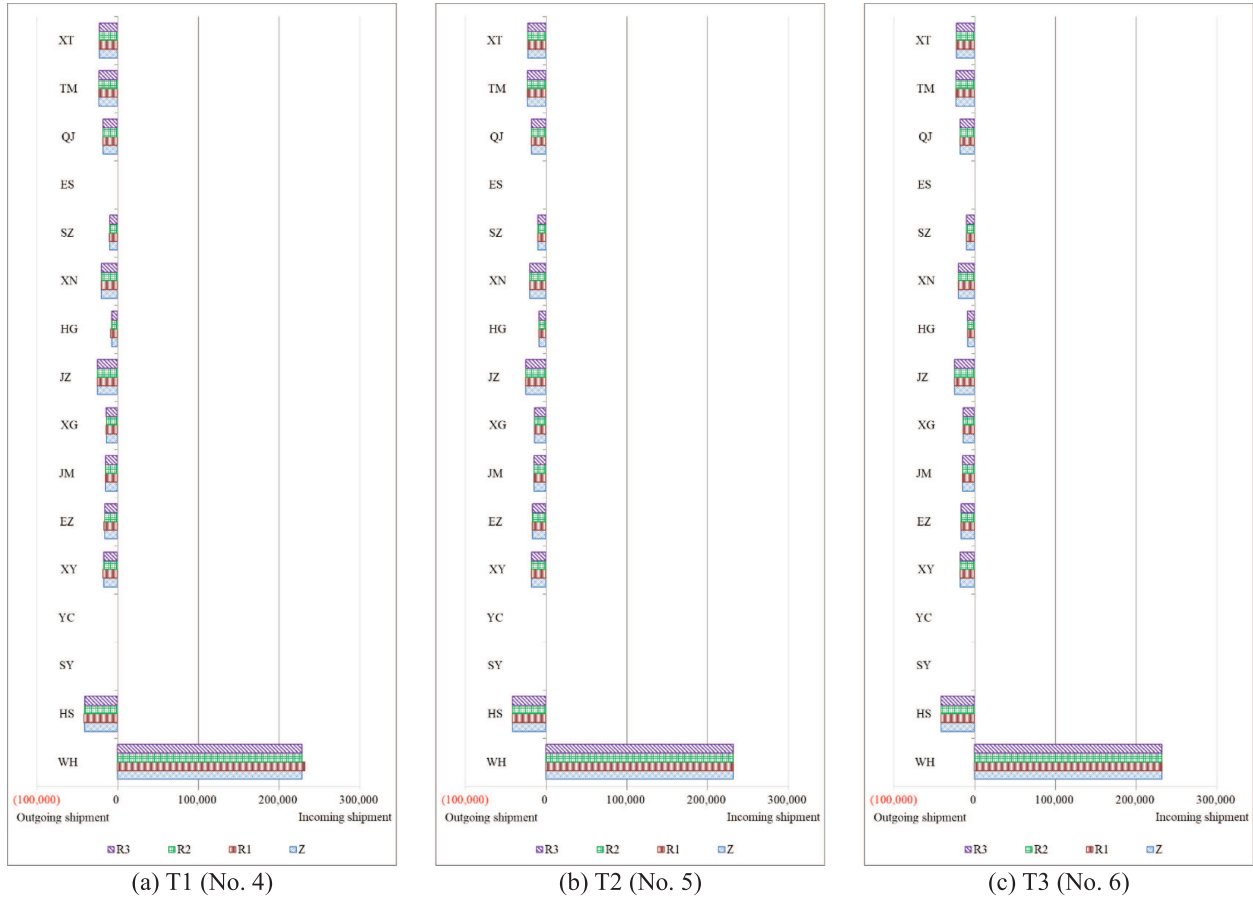


FIGURE 6. Medical supply rebalancing strategy without data contamination in Case C1.

traditional approaches like \mathcal{R}_1 in accuracy, underscoring their potential as reliable tools for medical supply rebalancing.

5.4. Numerical validation of the middle- and lower-level problem (Phase II) with outliers

Once we have acquired the optimal solutions to the MSPR problem in the absence of outliers, we can proceed to evaluate the performance of the proposed robust models in the presence of data contamination. To do so, this study employs a conventional robust estimator and introduces two novel robust estimators aimed at mitigating the influence of outliers within the MSPR problem. In this assessment, we assume the presence of an outlier (denoted as φ) within the first scenario realization in two typical regions (WH and HG). This outlier is significantly larger or smaller than the other potential demand quantities. Subsequently, this study employs the medical supply flows and quantifies the outgoing/incoming shipments in these two regions to assess the robustness of the proposed models.

(1) Demand with an outlier in WH

To investigate and validate the robustness of the proposed models, a numerical instance of Case C2 was tested under three probability types. In this analysis, this study modified the outlier value in the demand for medical supplies in WH ($\varphi = \phi A_{tw1}$ and $\phi > 0$). The quantities of incoming shipments at WH for various outlier

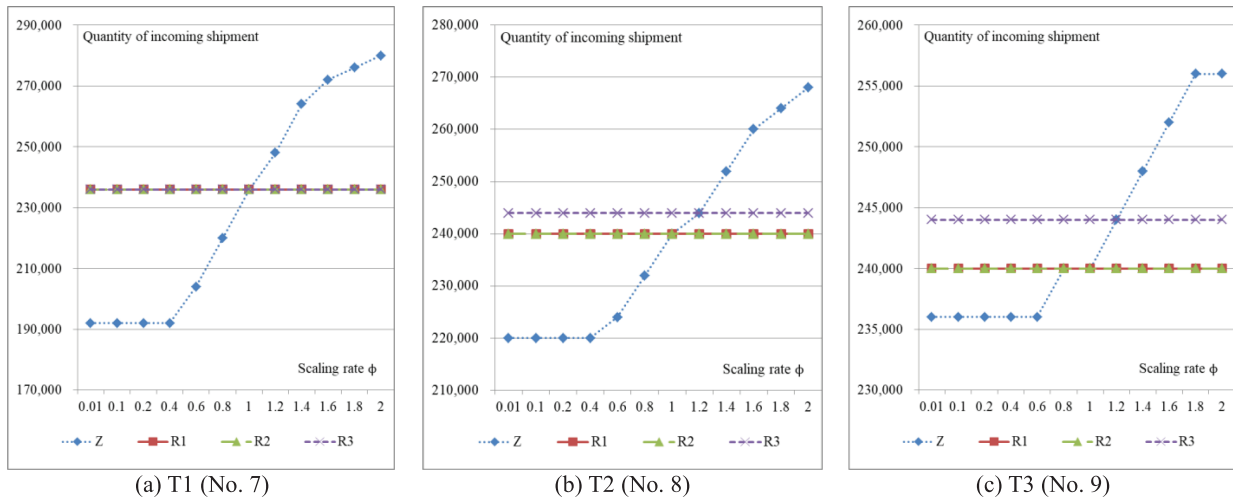


FIGURE 8. Robust property comparison of four models (\mathcal{Z} , \mathcal{R}_1 , \mathcal{R}_2 , and \mathcal{R}_3) with an outlier in demand at WH.

values are illustrated in Figure 8. It is evident from the figure that the quantity of incoming shipments at WH increases as the outlier value grows from $\phi = 0.01$ when model \mathcal{Z} is used, indicating a substantial impact of outlier values on the medical supply rebalancing strategy under this model. However, when the proposed robust models are employed, the quantities of incoming shipments at WH exhibit a stable trend with increasing outlier values. This observation underscores the superior performance of the proposed robust models compared to the traditional stochastic optimization model.

Additionally, to illustrate the impact of an outlier in the demand for medical supplies in WH across the three probability types, we present the medical supply rebalancing strategy along with the optimal medical supply flows in Figure 9. In this graphical representation, regions with longer string indicators denote supply points, whereas those with shorter string indicators denote demand points, providing a clear visual distinction of their respective roles in the supply network. It is clearly observable from the figure that when data contamination, specifically an extreme outlier in WH’s demand, is introduced, the network structure undergoes significant and counterintuitive changes. For instance, the region XY erroneously becomes a demand point, as evidenced in both Figures 9a and 9b. This discrepancy arises because the demand for medical supplies at WH diminishes significantly, reflecting an extremely small realization (contaminated scenario) within its uncertain demand set ($\phi = 0.01$). Consequently, the model perceives WH as having minimal or negligible need for supplies, which in turn causes XY to be incorrectly classified as a demand point in the rebalancing strategy. Moreover, both incoming and outgoing shipments in these 16 regions undergo substantial adjustments when data contamination is taken into account at WH (as shown in Fig. 9). These adjustments reflect the proposed model attempting to re-optimize the supply flows in response to the erroneous demand information, leading to potentially inefficient or suboptimal allocation of resources throughout the network. Nevertheless, the proposed models (\mathcal{R}_1 , \mathcal{R}_2 , and \mathcal{R}_3) exhibit robust outlier-resistant properties, primarily due to their robust estimators, when dealing with contaminated demand for medical supplies, as exemplified in the case of WH. In conclusion, this case study exemplifies how outliers in regional demand can substantially disrupt the optimal supply rebalancing strategy if left unaddressed. It also highlights the importance and effectiveness of the proposed robust models in safeguarding the decision-making process against data contamination, ensuring more reliable and resilient outcomes even under adverse conditions.

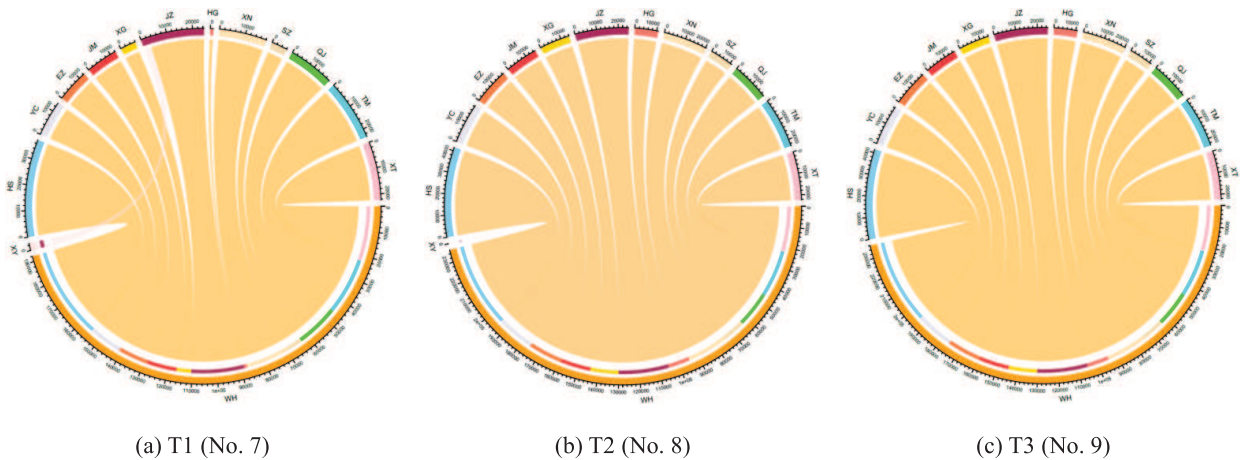


FIGURE 9. Medical supply rebalancing strategy with the medical supply-flows with model \mathcal{Z} and $\phi = 0.01$.

(2) Demand with an outlier in HG

This study further delves into the impact of outliers on outgoing shipments at a supply point (HG) under the assumption that an outlier exists in the uncertain demand for medical supplies in HG. Figure 10 illustrates the quantities of outgoing and incoming shipments at HG across different outlier values. It is evident that HG is initially classified as a supply point due to its low demand for medical supplies. However, as the outlier value increases, HG undergoes a transformation into a demand point, receiving medical supplies from other regions. Notably, outliers exert a substantial influence on the quantities of outgoing and incoming shipments in HG. Nevertheless, upon the application of the proposed robust models, the quantities of outgoing shipments at HG exhibit a consistent trend, even with increasing outlier values. This observation validates the superior performance of the proposed robust models compared to the traditional stochastic optimization model.

Additionally, to more comprehensively illustrate the impact of an outlier in the demand for medical supplies at HG under the three probability types considered in this study, we present the corresponding medical supply rebalancing strategy along with the optimal medical supply flows in Figure 11. In this visual representation, regions marked with longer strings denote supply points, whereas those marked with shorter strings denote demand points, thereby facilitating a clear distinction between the two roles within the supply network. From Figure 11, it becomes apparent that when data contamination, an extreme outlier in HG demand, is introduced into the analysis, the overall rebalancing strategy of the network exhibits noticeable and somewhat counterintuitive changes. Partially, the region XY is erroneously reclassified as a demand point, as clearly illustrated in both Figures 11a and 11b. This discrepancy arises because the demand for medical supplies at WH diminishes significantly, reflecting an extremely small realization (contaminated scenario) within its uncertain demand set ($\phi = 0.01$). As a result, the model perceives WH as having negligible or even zero demand, thereby altering the supply-demand dynamics and misallocating the role of other regions, such as XY. Furthermore, as shown in Figure 11, the presence of this contaminated data at WH has broader repercussions for the entire supply network. Both incoming and outgoing shipments in these 16 regions undergo substantial adjustments when data contamination is taken into account at HG (as shown in Fig. 11). These adjustments reflect the proposed model attempting to rebalance the supply chain under incorrect assumptions about WH needs, which could lead to inefficiencies and potentially adverse outcomes in practice if such outliers are not properly accounted for. In conclusion, the proposed models (\mathcal{R}_1 , \mathcal{R}_2 , and \mathcal{R}_3) exhibit robust outlier-resistant properties, primarily due to their robust estimators, when dealing with contaminated demand for medical supplies, as exemplified in the case of HG.

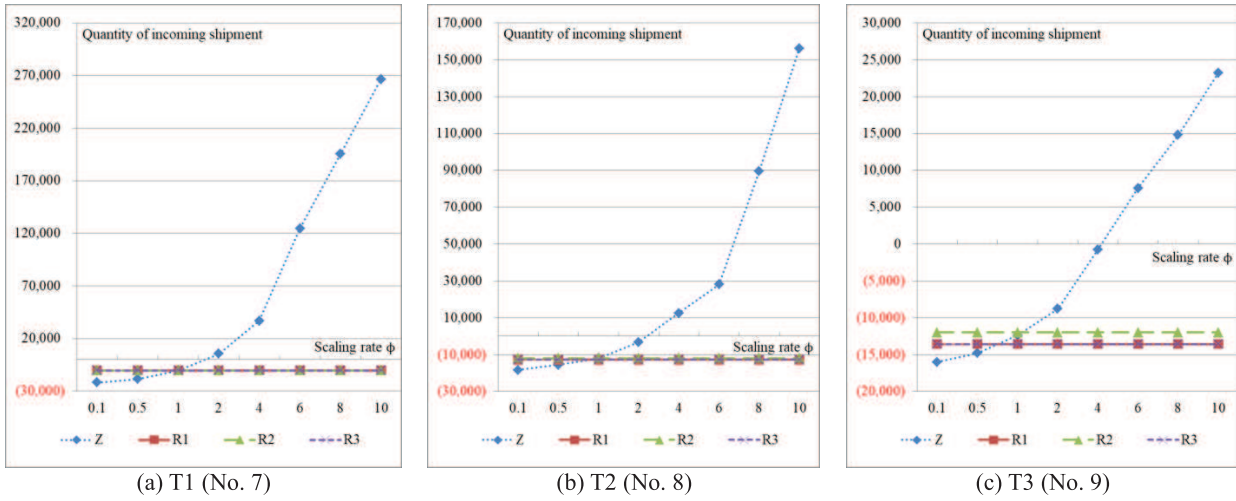


FIGURE 10. Robust property comparison of four models (\mathcal{L} , \mathcal{R}_1 , \mathcal{R}_2 , and \mathcal{R}_3) with an outlier in demand at HG.

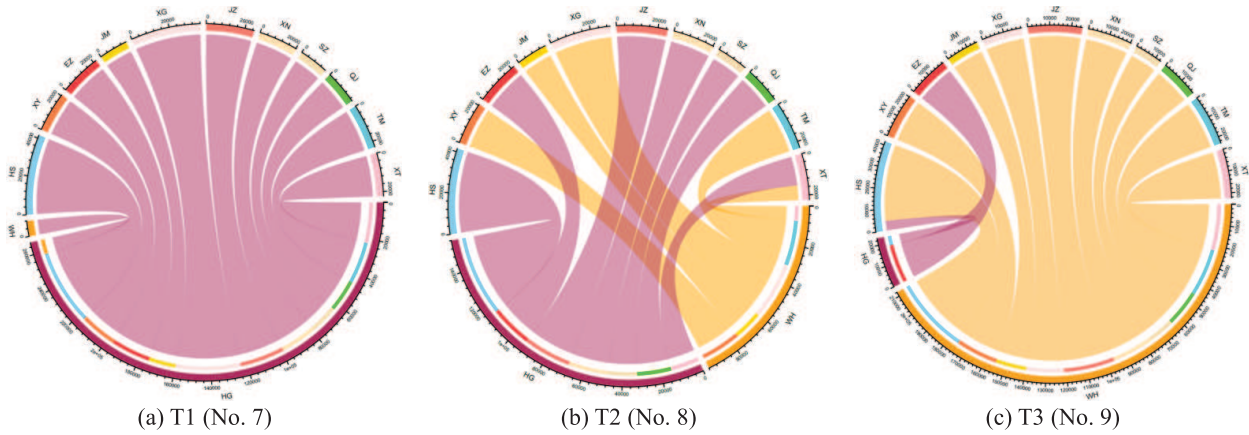


FIGURE 11. Medical supply rebalancing strategy with the medical supply-flows with model \mathcal{L} and $\phi = 10.0$.

5.5. Sensitivity analysis to additional supply

To analyze the impact of additional medical supplies after an epidemic on the medical supply rebalancing strategy, four different quantities of additional medical supplies were tested, excluding any consideration of outliers. These varying quantities of additional medical supplies are specifically allocated to directly support WH, given its exceptionally high and urgent demand in the post-epidemic period. This design reflects a realistic and critical decision-making context, where a severely affected region is prioritized for external aid to stabilize the overall supply-demand balance.

This section delves into the medical supply rebalancing strategy across these 16 regions under different quantities of additional medical supplies. The strategies, complete with medical supply flows, are presented in Figure 12. Figure 12a reveals that with an additional 100 000 units of medical supplies, both WH and YC are designated as demand points. As the quantity of additional medical supplies increases progressively from

Second, this study assumes that the probabilities of scenarios are uniform across all areas to reflect the lack of prior knowledge about the spatial distribution of epidemic outbreaks during the early response phase. This assumption also facilitates the tractability and clarity of the proposed mathematical models. Nevertheless, alternative probability distributions, such as those weighted by population density, historical infection rates, or risk exposure levels, could also be considered to better capture heterogeneity across regions. Incorporating non-uniform probabilities would likely shift more resources toward higher-risk areas and fewer to lower-risk ones, resulting in different repositioning and rebalancing strategies.

Third, this study underscores the necessity of incorporating robust optimization methods into decision-making processes. Real-world data in emergency contexts are often noisy, incomplete, or even misleading due to reporting delays, measurement errors, or unexpected anomalies. Robust optimization techniques enhance the resilience of allocation plans by accounting for such irregularities, thereby preventing misallocation of resources, inefficiencies, and even failures of the supply chain. At the same time, numerical experiments demonstrate that all instances can be solved efficiently within few seconds on standard hardware, which confirms the practical feasibility of our approach. Managers who proactively implement robust, outlier-resistant models will be better positioned to maintain stability and continuity of operations under adverse conditions.

Moreover, the findings from sensitivity analyses highlight the value of timely and sufficient external supply supplementation. When critical regions face overwhelming demand, external support not only alleviates the immediate burden on these regions but also allows for a more balanced and equitable redistribution of resources across the network. This reduces the risks and uncertainties associated with interregional sharing of limited resources and helps sustain the overall functionality of the supply chain.

In addition, the computational complexity of the proposed three-level optimization framework deserves attention. Thanks to the linearization techniques applied to the upper-level problem and the incorporation of robust estimators in the middle- and lower-level problems, the models remain computationally tractable. Our numerical experiments demonstrate that all tested instances can be solved efficiently within few seconds on standard computing hardware, suggesting that the proposed approach is suitable for practical decision-making scenarios. However, it should be noted that as the number of regions, scenarios, or decision variables increases, the problem size and solution time may grow accordingly. In such cases, advanced techniques such as decomposition methods, parallel computation, or heuristic algorithms could be explored to further enhance scalability and efficiency.

Therefore, managers are strongly encouraged to integrate robust optimization-based decision tools with dynamic, real-time data streams to design adaptive and scientifically grounded supply allocation strategies. At the same time, strengthening interregional coordination mechanisms and enhancing the speed and flexibility of emergency supply dispatch are vital for building a more resilient and responsive public health emergency system. By implementing these recommendations, managers can improve not only the efficiency and equity of resource allocation but also the broader resilience of health systems to withstand and recover from large-scale crises.

6. CONCLUSIONS

This study delves deeply into the MSPR problem, particularly focusing on the challenge posed by data contamination in response to epidemics, a fact that has hitherto remained unexplored. To mitigate the adverse effects of data contamination, two novel robust optimization models have been proposed. These models are designed as tri-level multi-objective optimization models, incorporating the influential concept of the law of DMU to optimize the medical supply repositioning and rebalancing processes. Comparative analyses of the optimal solutions demonstrate the outlier-resistant performance of these robust optimization models. To enable a unique MSPR scheme, this study has also developed corresponding linearization techniques. A real case study, centered on the COVID-19 outbreak in Hubei Province, has been implemented to validate the efficacy of the proposed methods. In this context, the newly proposed robust estimators have been evaluated alongside existing ones, and the proposed robust optimization models have been compared with traditional stochastic optimization

models, accounting for data contamination. Furthermore, actionable insights and managerial implications have been derived from the numerical instances within the case study, and these findings are summarized as follows:

- (i) Addressing the MSPR problem is crucial for rectifying the demand-supply imbalance during epidemic responses. As evident in Figures 6 and 7, WH faces a dire need for medical supplies compared to other regions. The stocked medical supplies in WH remain insufficient due to the substantial number of newly infected cases. Effective estimation of medical supply demand is imperative, and the medical supply rebalancing process plays a pivotal role in rectifying the demand-supply mismatch. Failure to address this imbalance can lead to a collapse of the healthcare system when viral transmission is uncontrolled.
- (ii) The proposed robust optimization models (\mathcal{R}_1 , \mathcal{R}_2 , and \mathcal{R}_3) outperform traditional stochastic optimization models in dealing with the MSPR problem in the presence of outliers. The numerical analysis of the case study indicates that optimal solutions obtained from models \mathcal{R}_2 and \mathcal{R}_3 closely approach the true optimum compared to model \mathcal{R}_1 . Models \mathcal{R}_2 and \mathcal{R}_3 incorporate weights, enhancing their ability to handle the impact of data contamination (see Figs. 8–11). Consequently, the proposed robust mathematical models are indispensable for mitigating the effects of data contamination within the MSPR problem.

In addition to these notable contributions, this study has its limitations. It primarily focuses on the single-period MSPR problem with data contamination in response to epidemics and does not encompass medical supply operations aimed at supporting medical staff post-epidemic. Future research directions may encompass: Investigation of a more robust multi-period MSPR strategy, accounting for dynamic and extended-duration scenarios. Consideration of medical supply operations supporting medical staff, a more intricate challenge that necessitates the clarification of the relationship between patient numbers and medical staff requirements.

FUNDING

This work was supported by the National Natural Science Foundation of China with Grant Nos. 72104020 and 72574017 and the National Research Foundation of Korea (NRF) grant funded by the Korea government (MSIT) (Nos. 2022R1A2C1091319 and RS-2023-00242528).

REFERENCES

- [1] M. Akbarpour, S.A. Torabi and A. Ghavamifar, Designing an integrated pharmaceutical relief chain network under demand uncertainty. *Transp. Res. Part E: Logistics Transp. Rev.* **136** (2020) 101867.
- [2] D. Alem, H.F. Bonilla-Londono, A.P. Barbosa-Povoa, S. Relvas, D. Ferreira and A. Moreno, Building disaster preparedness and response capacity in humanitarian supply chains using the Social Vulnerability Index. *Eur. J. Oper. Res.* **292** (2021) 250–275.
- [3] A. Amjadian and A. Gharaei, An integrated reliable five-level closed-loop supply chain with multi-stage products under quality control and green policies: generalised outer approximation with exact penalty. *Int. J. Syst. Sci.: Oper. Logistics* **9** (2022) 429–449.
- [4] A.N. Arnette and C.W. Zobel, A risk-based approach to improving disaster relief asset pre-positioning. *Prod. Oper. Manage.* **28** (2019) 457–478.
- [5] C. Ash, C. Diallo, U. Venkatadri and P. VanBerkel, Distributionally robust optimization of a Canadian healthcare supply chain to enhance resilience during the COVID-19 pandemic. *Comput. Ind. Eng.* **168** (2022) 108051.
- [6] H. Baharmand, T. Comes and M. Lauras, Bi-objective multi-layer location–allocation model for the immediate aftermath of sudden-onset disasters. *Transp. Res. Part E: Logistics Transp. Rev.* **127** (2019) 86–110.
- [7] B. Balcik, S. Silvestri, M.È. Rancourt and G. Laporte, Collaborative Prepositioning network design for regional disaster response. *Prod. Oper. Manage.* **28** (2019) 2431–2455.
- [8] C. Cao, Y. Liu, O. Tang and X. Gao, A fuzzy bi-level optimization model for multi-period post-disaster relief distribution in sustainable humanitarian supply chains. *Int. J. Prod. Econ.* **235** (2021) 108081.
- [9] C. Cao, J. Liu, W. Liu, M.C. Chou, F. Zhang and Y. Zhang, Location and transportation joint decisions for infectious medical waste in sustainable supply chains during a pandemic: a bi-level optimization approach. *Ann. Oper. Res.* (2025) 1–49.

- [10] F. Cavdur, M. Kose-Kucuk and A. Sebatli, Allocation of temporary disaster response facilities under demand uncertainty: an earthquake case study. *Int. J. Disaster Risk Reduction* **19** (2016) 159–166.
- [11] Y. Chen, Q. Zhao, K. Huang and X. Xi, A Bi-objective optimization model for contract design of humanitarian relief goods procurement considering extreme disasters. *Soc.-Econ. Planning Sci.* **81** (2022) 101214.
- [12] C. Cheng, Y. Adulyasak and L.M. Rousseau, Robust facility location under demand uncertainty and facility disruptions. *Omega* **103** (2021) 102429.
- [13] A. Dhungana, E.H. Doyle, G. McDonald and R. Prasanna, Navigating scientific modelling and uncertainty: insights from hazard, risk, and impact scientists in disaster risk management (DRM). *Int. J. Disaster Risk Reduction* **118** (2025) 105260.
- [14] Z. Dönmez, B.Y. Kara, Ö. Karsu and F. Saldanha-da-Gama, Humanitarian facility location under uncertainty: critical review and future prospects. *Omega* **102** (2021) 102393.
- [15] B. Ehsani, H. Karimi, A. Bakhshi, A. Aghsami and M. Rabbani, Designing humanitarian logistics network for managing epidemic outbreaks in disasters using Internet-of-Things. A case study: an earthquake in Salas-e-Babajani city. *Comput. Ind. Eng.* **175** (2023) 108821.
- [16] S. Enayati and O.Y. Özaltın, Optimal influenza vaccine distribution with equity. *Eur. J. Oper. Res.* **283** (2020) 714–725.
- [17] G. Erbeyoğlu and Ü. Bilge, A robust disaster preparedness model for effective and fair disaster response. *Eur. J. Oper. Res.* **280** (2020) 479–494.
- [18] X. Gao, Determination of the Optimal Facility Location based on the Minimum Distance Approach. Pusan National University (2020).
- [19] X. Gao, A bi-level stochastic optimization model for multi-commodity rebalancing under uncertainty in disaster response. *Ann. Oper. Res.* **319** (2022) 115–148.
- [20] X. Gao and C. Cao, Multi-commodity rebalancing and transportation planning considering traffic congestion and uncertainties in disaster response. *Comput. Ind. Eng.* **149** (2020) 106782.
- [21] X. Gao and C. Cui, A note on the warehouse location problem with data contamination. *RAIRO-Oper. Res.* **55** (2021) 1113–1135.
- [22] X. Gao and X. Jin, A robust multi-commodity rebalancing process in humanitarian logistics, in *Advances in Production Management System, APMS 2020*. Vol. 591. Springer, Cham (2020).
- [23] X. Gao, X. Jin, P. Zheng and C. Cui, Multi-modal transportation planning for multi-commodity rebalancing under uncertainty in humanitarian logistics. *Adv. Eng. Inf.* **47** (2021) 101223.
- [24] X. Gao, G. Huang, Q. Zhao, C. Cao and H. Jiang, Robust optimization model for medical staff rebalancing problem with data contamination during COVID-19 pandemic. *Int. J. Prod. Res.* **60** (2022) 1737–1766.
- [25] X. Gao, Z. Chen, B. Kim, and C. Park, A note on location parameter estimation using the weighted Hodges–Lehmann estimator. *Ind. Eng. Manage. Syst.* **23** (2024) 323–341.
- [26] A. Gharaei, A. Amjadian, A. Shavandi and A. Amjadian, An augmented Lagrangian approach with general constraints to solve nonlinear models of the large-scale reliable inventory systems. *J. Comb. Optim.* **45** (2023) 78.
- [27] A. Gharaei, A. Amjadian, M.V. Sebt and E.B. Tirkolaee, Single-vendor single-buyer multi-product economic production quantity problem with stochastic constraints: a modified generalized elimination method. *J. Oper. Res. Soc.* **76** (2025) 1047–1065.
- [28] J.L. Hodges and E.L. Lehmann, Estimates of location based on rank tests. *Ann. Math. Stat.* (1963) 598–611.
- [29] X. Hong, M.A. Lejeune and N. Noyan, Stochastic network design for disaster preparedness. *IIE Trans.* **47** (2015) 329–357.
- [30] S. Hu, and Z.S. Dong, Supplier selection and pre-positioning strategy in humanitarian relief. *Omega* **83** (2019) 287–298.
- [31] Z. Hu, C. Song, C. Xu, G. Jin, Y. Chen, X. Xu, H. Ma, W. Chen, Y. Lin, Y. Zheng and J. Wang, Clinical characteristics of 24 asymptomatic infections with COVID-19 screened among close contacts in Nanjing, China. *Sci. Chin. Life Sci.* **63** (2020) 706–711.
- [32] M. Khoshsirar, R. Dabbagh and A. Bozorgi-Amiri, A multi-objective robust possibilistic programming approach to coordinating procurement operations in the disaster supply chain using a multi-attribute reverse auction mechanism. *Comput. Ind. Eng.* **158** (2021) 107414.
- [33] Y. Liu, H. Lei, Z. Wu and D. Zhang, A robust model predictive control approach for post-disaster relief distribution. *Comput. Ind. Eng.* **135** (2019) 1253–1270.
- [34] K. Liu, Q. Li and Z.H. Zhang, Distributionally robust optimization of an emergency medical service station location and sizing problem with joint chance constraints. *Transp. Res. Part B: Methodol.* **119** (2019) 79–101.

- [35] L. Liu, Y. Ma, C. Park and J.H. Byun, Robust sequential bifurcation for simulation factor screening under data contamination. *Comput. Ind. Eng.* **129** (2019) 102–112.
- [36] K. Liu, H. Zhang and Z.H. Zhang, The efficiency, equity and effectiveness of location strategies in humanitarian logistics: a robust chance-constrained approach. *Transp. Res. Part E: Logistics Transp. Rev.* **156** (2021) 102521.
- [37] K. Liu, C. Liu, X. Xiang and Z. Tian, Testing facility location and dynamic capacity planning for pandemics with demand uncertainty. *Eur. J. Oper. Res.* **304** (2023) 150–168.
- [38] A. Nagurney, E.A. Flores and C. Soyly, A generalized Nash equilibrium network model for post-disaster humanitarian relief. *Transp. Res. Part E: Logistics Transp. Rev.* **95** (2016) 1–18.
- [39] W. Ni, J. Shu and M. Song, Location and emergency inventory pre-positioning for disaster response operations: Min-max robust model and a case study of Yushu earthquake. *Prod. Oper. Manage.* **27** (2018) 160–183.
- [40] L. Ouyang, J. Chen, Y. Ma, C. Park and J. Jin, Bayesian closed-loop robust process design considering model uncertainty and data quality. *IIE Trans.* **52** (2020) 288–300.
- [41] D. Pamucar, A.E. Torkayesh and S. Biswas, Supplier selection in healthcare supply chain management during the COVID-19 pandemic: a novel fuzzy rough decision-making approach. *Ann. Oper. Res.* **328** (2023) 977–1019.
- [42] K.E. Paret, M.E. Mayorga and E.J. Lodree, Assigning spontaneous volunteers to relief efforts under uncertainty in task demand and volunteer availability. *Omega* **99** (2021) 102228.
- [43] C. Park, Determination of the joint confidence region of the optimal operating conditions in robust design by the bootstrap technique. *Int. J. Prod. Res.* **51** (2013) 4695–4703.
- [44] C. Park and M. Leeds, A highly efficient robust design under data contamination. *Comput. Ind. Eng.* **93** (2016) 131–142.
- [45] C. Park, L. Ouyang, J.H. Byun and M. Leeds, Robust design under normal model departure. *Comput. Ind. Eng.* **113** (2017) 206–220.
- [46] C. Park, H. Kim and M. Wang, Investigation of finite-sample properties of robust location and scale estimators. *Commun. Stat. Simul. Comput.* **51** (2022) 2619–2645.
- [47] C. Park, X. Gao and M. Wang, Robust explicit estimators using the power-weighted repeated medians. *J. Appl. Stat.* **51** (2024) 1590–1608.
- [48] S.K. Paul, M.A. Moktadir, K. Sallam, T.M. Choi and R.K. Chakraborty, A recovery planning model for online business operations under the COVID-19 outbreak. *Int. J. Prod. Res.* **61** (2023) 2613–2635.
- [49] K. Ransikarbum and S.J. Mason, A bi-objective optimisation of post-disaster relief distribution and short-term network restoration using hybrid NSGA-II algorithm. *Int. J. Prod. Res.* **60** (2022) 5769–5793.
- [50] A. Sadeghi, F. Aros-Vera, H. Mosadegh and R. YounesSinaki, Social cost-vehicle routing problem and its application to the delivery of water in post-disaster humanitarian logistics. *Transp. Res. Part E: Logistics Transp. Rev.* **176** (2023) 103189.
- [51] M. Schoonhoven, H.Z. Nazir, M. Riaz and R.J. Does, Robust location estimators for the \bar{U} control chart. *J. Qual. Technol.* **43** (2011) 363–379.
- [52] I. Shokr, F. Jolai and A. Bozorgi-Amiri, A novel humanitarian and private sector relief chain network design model for disaster response. *Int. J. Disaster Risk Reduction* **65** (2021) 102522.
- [53] J.M. Stauffer, A.J. Pedraza-Martinez, L.L. Yan and L.N. Van Wassenhove, Asset supply networks in humanitarian operations: a combined empirical-simulation approach. *J. Oper. Manage.* **63** (2018) 44–58.
- [54] V.F. Stienen, J.C. Wagenaar, D. Den Hertog and H.A. Fleuren, Optimal depot locations for humanitarian logistics service providers using robust optimization. *Omega* **104** (2021) 102494.
- [55] A.A. Taleizadeh, A. Amjadian, S.E. Hashemi-Petroodi and I. Moon, Supply chain coordination based on mean-variance risk optimisation: pricing, warranty, and full-refund decisions. *Int. J. Syst. Sci.: Oper. Logistics* **10** (2023) 2249808.
- [56] M. Wang, J. Zhao, X. Sun and C. Park, Robust explicit estimation of the two-parameter Birnbaum–Saunders distribution. *J. Appl. Stat.* **40** (2013) 2259–2274.
- [57] M. Wang, C. Park and X. Sun, Simple robust parameter estimation for the Birnbaum–Saunders distribution. *J. Stat. Distrib. App.* **2** (2015) 14.
- [58] W. Wang, K. Yang, L. Yang and Z. Gao, Two-stage distributionally robust programming based on worst-case mean-CVaR criterion and application to disaster relief management. *Transp. Res. Part E: Logistics Transp. Rev.* **149** (2021) 102332.
- [59] Q. Wang, Y. Liu, and H. Pei, Modelling a bi-level multi-objective post-disaster humanitarian relief logistics network design problem under uncertainty. *Eng. Optim.* **56** (2024) 1220–1254.

- [60] Z. Wang, K. Liu, K. You and Z. Wang, Wasserstein distributionally robust facility location and capacity planning for disaster relief. *Expert Syst. App.* **272** (2025) 126647.
- [61] Y. Yang, Y. Yin, D. Wang, J. Ignatius, T.C.E. Cheng and L. Dhamotharan, Distributionally robust multi-period location-allocation with multiple resources and capacity levels in humanitarian logistics. *Eur. J. Oper. Res.* **305** (2023) 1042–1062.
- [62] P. Zhang, Y. Liu, G. Yang and G. Zhang, A distributionally robust optimization model for designing humanitarian relief network with resource reallocation. *Soft Comput.* **24** (2020) 2749–2767.
- [63] W. Zhang, X. Shi, A. Huang, G. Hua and R.H. Teunter, Optimal stock and capital reserve policies for emergency medical supplies against epidemic outbreaks. *Eur. J. Oper. Res.* **304** (2023) 183–191.



Please help to maintain this journal in open access!

This journal is currently published in open access under the Subscribe to Open model (S2O). We are thankful to our subscribers and supporters for making it possible to publish this journal in open access in the current year, free of charge for authors and readers.

Check with your library that it subscribes to the journal, or consider making a personal donation to the S2O programme by contacting subscribers@edpsciences.org.

More information, including a list of supporters and financial transparency reports, is available at <https://edpsciences.org/en/subscribe-to-open-s2o>.